American Journal of Botany 101(2): 225–243. 2014.

Floral structure and development in Rafflesiaceae with emphasis on their exceptional gynoecia[1]

Lachezar A. Nikolov[2], Yannick M. Staedler[3], Sugumaran Manickam[4], Jürg Schönenberger[3], Peter K. Endress[5], Elena M. Kramer[2], and Charles C. Davis[2,6]

[2]Department of Organismic and Evolutionary Biology, Harvard University Herbaria, Cambridge, Massachusetts 02138 USA; [3]Department of Structural and Functional Botany, Faculty Centre of Biodiversity, Rennweg 14, A-1030, Wien, Austria; [4]Rimba Ilmu Botanic Garden, Institute of Biological Sciences, University of Malaya 50603 Kuala Lumpur, Malaysia; and [5]Institute of Systematic Botany, University of Zurich, Zollikerstrasse 107, CH-8008 Zurich, Switzerland

- *Premise of the study:* The holoparasitic plant family Rafflesiaceae include the world's largest flowers. Despite their iconic status, relatively little is known about the morphology and development of their flowers. A recent study clarified the organization of the outer (sterile) floral organs, surprisingly revealing that their distinctive floral chambers arose via different developmental pathways in the two major genera of the family. Here, we expand that research to investigate the structure and development of the reproductive organs of Rafflesiaceae.
- *Methods:* Serial sectioning, scanning electron microscopy, and x-ray tomography of floral buds were employed to reconstruct the structure and development of all three Rafflesiaceae genera.
- *Key results:* Unlike most angiosperms, which form their shoot apex from the primary morphological surface, the shoot apex of Rafflesiaceae instead forms secondarily via internal cell separation (schizogeny) along the distal boundary of the host–parasite interface. Similarly, the radially directed ovarial clefts of the gynoecium forms via schizogeny within solid tissue, and no carpels are initiated from the floral apex.
- *Conclusions:* The development of the shoot apex and gynoecium of Rafflesiaceae are highly unusual. Although secondary formation of the morphological surface from the shoot apex has been documented in other plant groups, secondary derivation of the inner gynoecium surface is otherwise unknown. Both features are likely synapomorphies of Rafflesiaceae. The secondary derivation of the shoot apex may protect the developing floral shoot as it emerges from within dense host tissue. The secondary formation of the ovarial clefts may generate the extensive placental area necessary to produce hundreds of thousands of ovules.

Key words: androecium; floral anatomy; floral development; gynoecium; *Rafflesia*; Rafflesiaceae; *Rhizanthes*; *Sapria*; shoot apex.

Rafflesiaceae are a family of holoparasitic endophytes that exhibit extreme modifications of their vegetative and reproductive bodies. They possess among the most reduced vegetative body of all angiosperms, having no readily identifiable roots and only a highly modified mycelium-like body consisting of a strand of cells plus the bracts that precede their flowers (L. A. Nikolov et al., unpublished data). At the same time, members of the family also produce the world's largest flowers (i.e., flowers in *Rafflesia arnoldii* R. Br. measure up to 1 m in diameter). These extremes have puzzled morphologists for nearly two centuries (Brown, 1822, 1845; Griffith, 1845). Interpretations of their bizarre morphology are problematic and have resulted in great confusion regarding both the evolutionary affinities of the group and the development of their remarkable body plan (Kuijt, 1969). Rafflesiaceae s.l. has traditionally included most endophytic angiosperms, which live vegetatively inside their obligate hosts. This broad circumscription included both the large-flowered *Rafflesia*, *Rhizanthes*, and *Sapria*, and the more moderately (to tiny-) sized *Cytinus*, *Bdallophyton*, *Mitrastema*, *Pilostyles*, and *Apodanthes* (Cronquist, 1988; Takhtajan, 1997). Recent phylogenetic evidence has demonstrated that these members do not form a clade, which is corroborated by the tremendous variation in gross morphology and pollen diversity among these members (Takhtajan et al., 1985). This result indicates that this form of extreme parasitism has evolved at least four times independently among the former Rafflesiaceae s.l. (Barkman et al., 2004; Nickrent et al., 2004). Rafflesiaceae as they are now recognized in the strict sense include only the large-flowered genera, the sister clades *Rafflesia* and *Rhizanthes*, and *Sapria* (Fig. 1), which have been placed sister to Euphorbiaceae in the rosid order Malpighiales (Davis et al., 2007; Wurdack and Davis, 2009). This is especially puzzling because the closest relatives of Rafflesiaceae s.s. possess minute flowers. A more rigorous comparative study of the floral

[1]Manuscript received 5 January 2014; revision accepted 7 January 2014.

The authors thank S. Vessabutr and the staff at Queen Sirikit Botanic Garden for allowing access to *Sapria*, S.-Y. Wong and members of the Wong Laboratory for logistical support, M. Matthews for help with microtome sectioning, R. Hellmiss for graphical support, B. Angell for the illustrations, and K. Bomblies, D. Boufford, C. Extavour, W. Friedman, D. Haig, A. Knoll, S. Mathews, B. Tomlinson, and members of the Davis, Kramer, and Friedman laboratories for valuable discussions. Imaging support was provided by the Center for Microscopy and Image Analysis at the University of Zurich, and the Center for Nanoscale Systems at Harvard University. This research was supported by National Science Foundation (NSF) AToL grant to C.C.D. (DEB-0622764) and NSF grant DEB-1120243 to C.C.D. and E.M.K.

[6]Author for correspondence (e-mail: cdavis@oeb.harvard.edu)

doi:10.3732/ajb.1400009

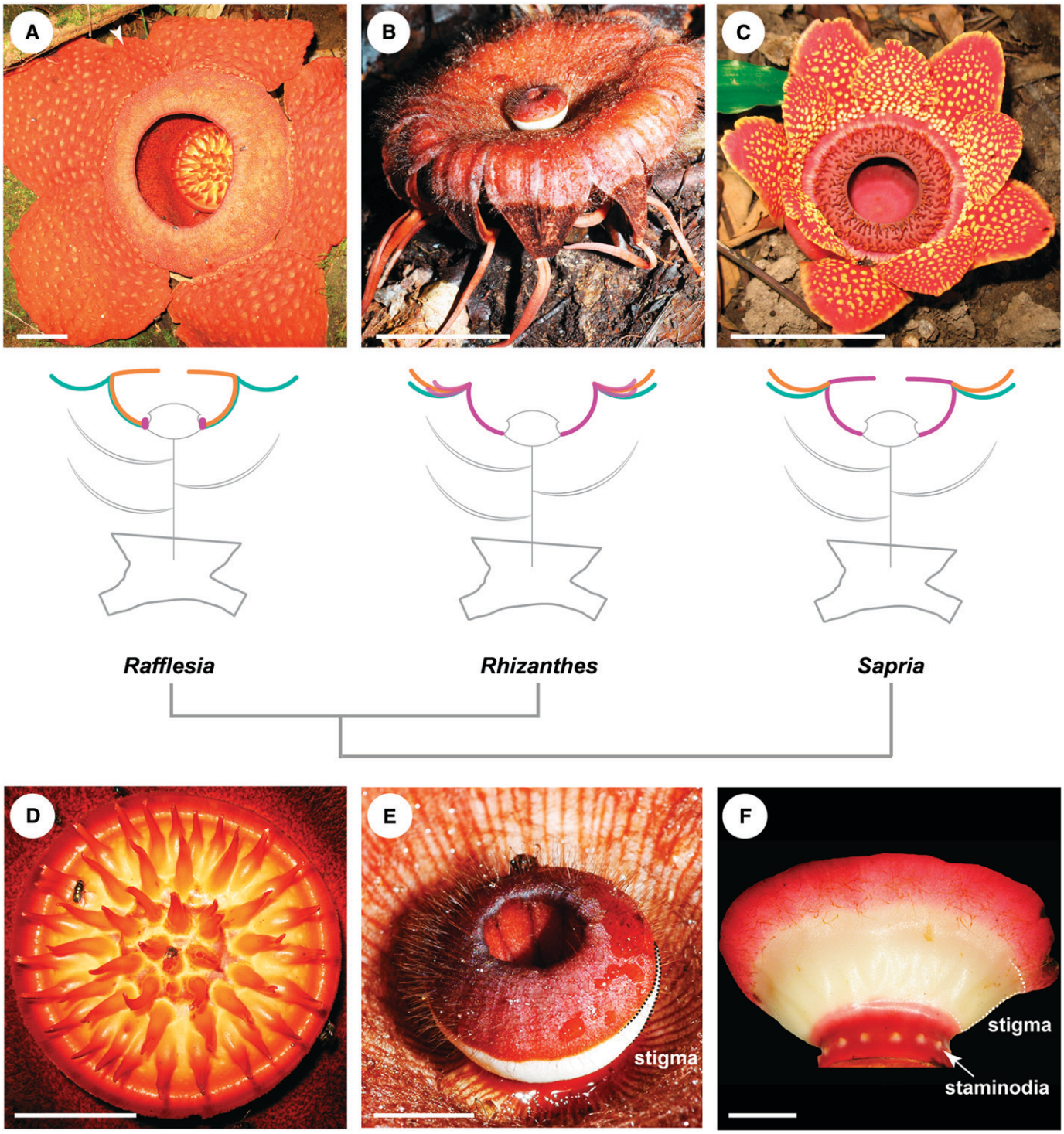

Fig. 1. Rafflesiaceae habit and gross morphology. (A–C) Below each photograph is a schematic of the floral organization in which a single flower emerges from the host (gray outline). Sepals are green, petals are orange, and the ring derivatives are in purple. Flowers of Rafflesiaceae are unisexual, but sex is not immediately obvious unless the undersurface of the central column is examined. (A) *Rafflesia tuan-mudae* anthetic flower. Note the rudimentary 6th perianth lobe (arrowhead). (B) *Rhizanthes lowii* anthetic flower. (C) *Sapria himalayana* anthetic flower. (D) *Rafflesia* central disk, top view. Note processes and carrion fly pollinators. (E) Central column of female *Rhizanthes lowii* flower. (F) Female *Sapria himalayana* central disk seen from the side. Dotted lines in (E) and (F) indicate the stigmatic surface. Bars: A–D = 10 cm; E and F = 1 cm.

morphology of Rafflesiaceae is needed to further investigate the dramatic transition between Rafflesiaceae and their small-flowered ancestors.

Rafflesia and *Sapria* are superficially very similar in having a conspicuous floral chamber—a partially occluded space confined by the perianth where the reproductive organs reside

TABLE 1. List of taxa and collections studied. Vouchers are deposited at Harvard University Herbaria, except for *Rafflesia patma* Blume (Botanical Institutes of the University of Zurich).

Taxon studied	Floral stage, sex	Material	Collection details
Rafflesia cantleyi Solms-Laubach	Floral buds, male and female	Liquid-fixed	C. Davis, 2007 L. Nikolov, 2011 (Buds A–O)
Rafflesia tuan-mudae Becc.	Floral buds, male and female	Liquid-fixed	C. Davis, 2007 L. Nikolov, 2011 (Buds A–L)
Rafflesia patma Blume	Floral buds, male and female	Liquid-fixed	A. Ernst, 1906
Rhizanthes lowii (Becc.) Harms	Floral buds, male and female	Liquid-fixed	C. Davis, 2007 L. Nikolov, 2011 (LN3440–3455)
Sapria himalayana Griffith	Floral buds, male and female	Liquid-fixed	L. Nikolov, 2011 (Buds A–Z)

(Fig. 1A, C). In *Rafflesia*, the perianth includes five perianth lobes, which appear to correspond to sepals in most angiosperms, and a congenitally fused petal whorl, which comprises the diaphragm that forms the roof of the chamber (Nikolov et al., 2013; Fig. 1A). Both perianth whorls serve protective and attractive functions. The perianth lobes and the diaphragm are congenitally fused at their bases to form the walls of the chamber known as the perianth tube. In contrast, *Sapria* has two free whorls each with five perianth lobes, corresponding to the sepal and the petal whorls, respectively (Nikolov et al., 2013; Fig. 1C). *Sapria* also possesses a diaphragm; however, this structure does not correspond to a canonical floral whorl. Instead, it is formed by the elaboration of a novel ring structure, which arises between the perianth and the androecium (Nikolov et al., 2013). Although such a ring structure is present in *Rafflesia*, it is relatively inconspicuous in advanced stages of floral development. Thus, despite their superficial similarities, the floral chambers are constructed differently in these two genera (Nikolov et al., 2013). These differences indicate that *Rafflesia*-like and *Sapria*-like floral chambers represent two distinct derivations of this morphology (Nikolov et al., 2013). The third genus, *Rhizanthes* (Fig. 1B), does not possess a floral chamber like *Rafflesia* and *Sapria*, but does exhibit expansion of the ring structure similar to *Sapria* (Nikolov et al., 2013). The main difference between the floral organization of *Sapria* and *Rhizanthes* lies in the elaboration of this ring structure. In *Sapria*, the ring forms the diaphragm, while in *Rhizanthes* the ring forms a series of pads that are congenitally fused to the adaxial surface of the perianth lobes (Nikolov et al., 2013; Fig. 1B, C). Given the placement of the early-diverging lineage containing *Sapria* and the sister relationship between *Rhizanthes* and *Rafflesia*, the presence of an elaborated ring structure likely represents the ancestral condition in the family (Nikolov et al., 2013). Thus, developmental repatterning identified in *Rafflesia* may have allowed their flowers to become even larger by providing a more rigid construction of the floral chamber (Nikolov et al., 2013). Specifically, the diaphragm may serve to reinforce the architecture of these giant flowers throughout development in forming a strut at the upper end of the perianth tube, which may function to support the large, heavy, sepal-derived perianth lobes.

The reproductive whorls in the three genera of Rafflesiaceae are organized into a conspicuous central column, which bears the fertile stamens or stigmatic surface in male and female flowers, respectively (Meijer, 1997) (Fig. 1D–F). The nature of this structure, however, has not been studied in detail. Shape and size of the central column do not vary significantly between male and female flowers. In all three genera, the central column has a neck-like constriction at its base that transitions into the receptacle, but additional elaborations differ among taxa. The column expands distally and forms a central disk in *Rafflesia* and *Sapria* (Meijer, 1997). The top surface of this disk is smooth in *Sapria*, but in *Rafflesia* it is crowned with many pronounced finger-like projections, called processes (Fig. 1D). In *Rhizanthes*, the central column is sharply concave and expands to a limited degree but does not form a broad central disk as in *Rafflesia* and *Sapria* (Bänziger and Hansen, 2000) (Fig. 1E). The flowers of Rafflesiaceae are usually unisexual by abortion—male flowers have vestigial ovaries, and reduced stamens are present in female flowers (Meijer, 1997) (Fig. 1F). Exceptional bisexual species of *Rafflesia* (*Ra. baletei* and *Ra. verrucosa*) have been discovered recently and also have been known in *Rhizanthes* for some time (Barcelona et al., 2006; Bänziger et al., 2007; Balete et al., 2010), but it remains to be determined whether these species are functionally bisexual. In the unisexual male flowers, a ring of stamens is located on the undersurface of the disk, while in female flowers, a stigmatic belt forms in a similar position (Beaman et al., 1988) (Fig. 1E, F). The ovary of female flowers is inferior, labyrinthine, with extensive intrusive placentae that bear numerous ovules. Aspects of the gynoecium development in the family were initially described by Solms-Laubach (1898) over a century ago and later by Ernst and Schmid (1913) and Hunziker (1926). According to these authors, the ovarial clefts form after cell separation (schizogeny) within solid tissue. In this case, the internal morphological surface of the carpels is not derived from the primary morphological surface of the floral apex (Endress, 2006, 2014). Schizogenous formation of the shoot apex in Rafflesiaceae stands in marked contrast to most angiosperms in which the shoot and floral apex are derived from a single continuous primary morphological surface that can be traced to the surface of the early-stage, globular embryo (Endress, 2006). Thus, the hypothesized condition in Rafflesiaceae is exceptional among angiosperms and controversial on theoretical grounds. Given this fact, we tested two additional models of gynoecium development that have some precedence in other taxa and seem consistent with the gross morphology of the female reproductive organs in Rafflesiaceae.

Here, we complement recent investigations on the morphology and development of the perianth of Rafflesiaceae (Nikolov et al., 2013) by focusing on the reproductive structures. In particular, we present a detailed study of floral meristem initiation and address outstanding questions regarding reproductive organ development, particularly the development of the gynoecium. Structural studies of Rafflesiaceae have been hampered by the sheer size of their flowers, which are not easily amenable to traditional microtechniques, particularly at later developmental stages. To overcome this obstacle, we used x-ray tomography, in addition to serial sectioning, and scanning electron microscopy. These high-resolution imaging techniques allow us to provide the first detailed description of the organization of the reproductive body of Rafflesiaceae and identify unifying developmental features in the family.

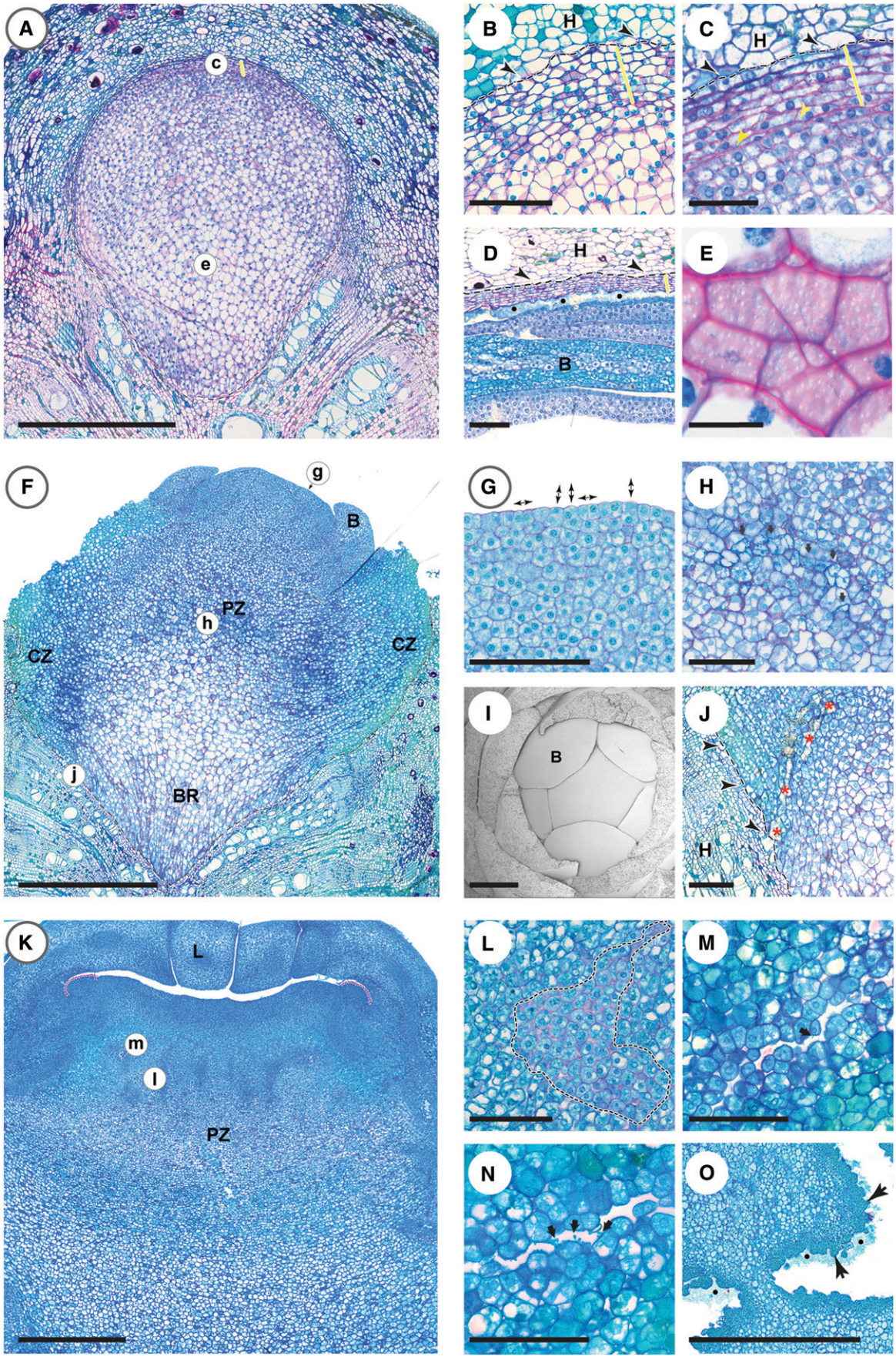
A
c
e
B
H
C
H
D
H
B
E
F
g
B
PZ
h
CZ
CZ
j
BR
G
H
I
B
J
H
K
L
m
l
PZ
L
M
N
O

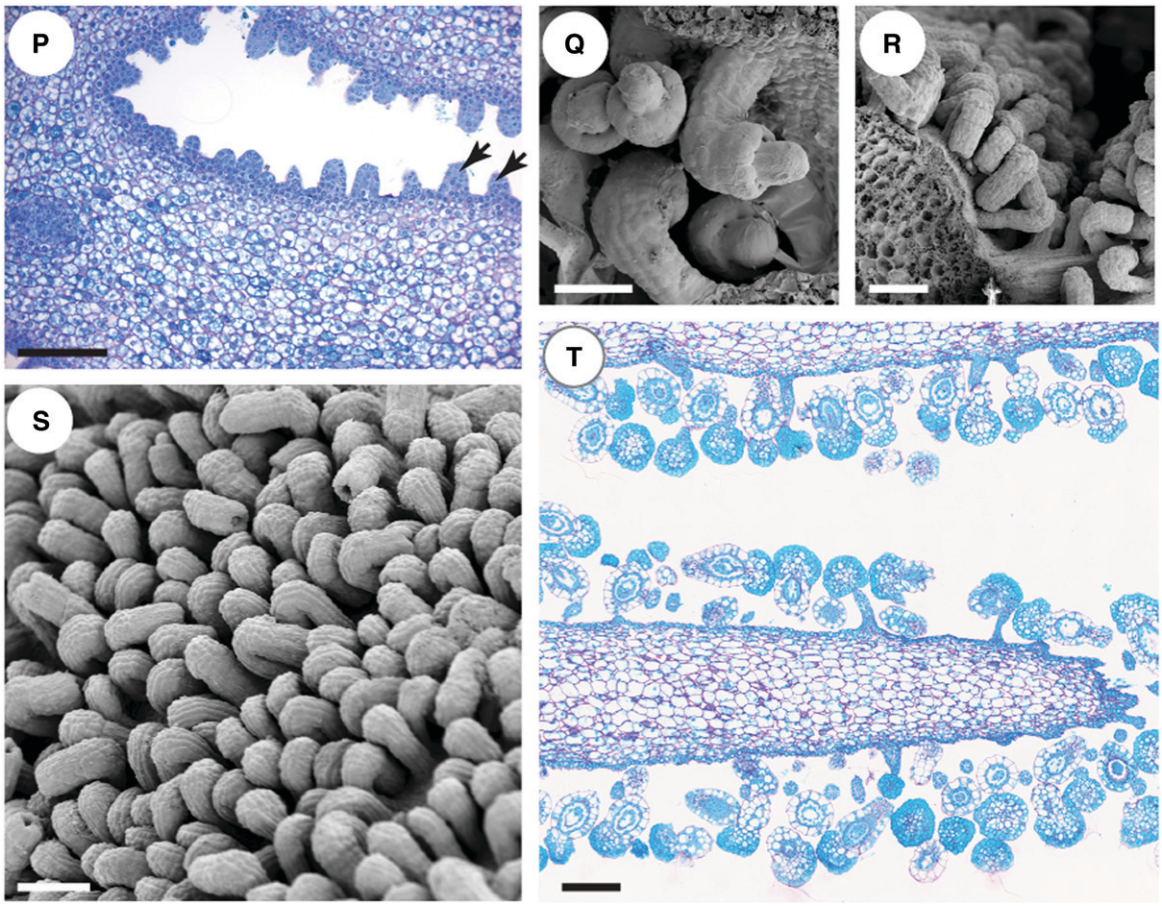

Fig. 2. Continued.

MATERIALS AND METHODS

Floral material—*Rafflesia cantleyi* Solms-Laubach and *Rafflesia tuan-mudae* Becc. buds were field collected in different developmental stages from low-elevation, humid dipterocarp forests in Ulu Geroh, Peninsular Malaysia and Gunung Puey, Sarawak, Borneo, respectively. *Sapria himalayana* Griffith was collected in the cloud forest in Queen Sirikit Botanic Garden, Chiang Mai, Thailand. *Rhizanthes lowii* (Becc.) Harms was collected from low-elevation primary rainforest near Kuching. Floral material for morphology was preserved in FAA (10% formalin, 5% acetic acid, 50% ethanol) for several days and stored in 70% ethanol thereafter. Vouchers are deposited in the Harvard University Herbaria (A). The historical collection of *Rafflesia patma* Blume by Alfred Ernst is housed at the Botanical Institutes of the University of Zurich (Z). The studied species are listed in Table 1.

Serial sectioning—Specimens for serial microtome sectioning were embedded in Kulzer's Technovit (2-hydroethyl methacrylate) (Igersheim and Cichocki, 1996). A stepwise infiltration was used with 50:50, 25:75, 0:100 ratios of

←

Fig. 2. Developing floral shoot histology of Rafflesiaceae, light microscopy, except I, Q, R, and S (SEM). All panels are *Rhizanthes lowii*, except for D, I, Q, R, and S (*Rafflesia cantleyi*). A, F, and K on the left are lower magnification images; circled lowercase letters illustrate regions, details of which are shown at a higher magnification in some of the uppercase panels on the right. (A) Teardrop-shaped protocorm, which has not emerged from the *Tetrastigma* host root; front marked with yellow bar. (B) Developing protocorm front as it appears at a stage earlier than (A), with initial differentiation of the leading cell layers (yellow bar). The interface between the host [H] and the parasite is depicted with a dashed line and black arrowheads. The parasite cells are easily recognizable by their larger nuclei. (C) Magnified region from (A), where the cells in the frontal zone (yellow bar) are flattened and cell separation has initiated (yellow arrowheads). Dashed line and black arrowheads depict the interface between the host [H] and the parasite. (D) A later stage than (A) where the front layer (yellow bar) has peeled off and the space between it and the bracts [B] is filled with mucilage (black dots). Dashed line depicts the interface between the host [H] and the parasite. (E) Basal region of the protocorm, with large cells and pronounced pit fields, suggesting extensive intercellular communication. (F) Shoot meristem with bract [B] initiation and positions of the pycnotic zone [PZ] and basal region [BR]. The region of the parasite adjacent to the host forms the contact zone [CZ]. (G) Shoot meristem and apex, where cells divide anticlinally (horizontal double arrows) and periclinally (vertical double arrows). (H) Pycnotic zone, cell inclusions are visible (arrows). (I) Shoot apex with spiral phyllotaxis of the bracts [B]. (J) Connection between the vasculature of the parasite (red asterisks) and the host [H]. The interface between host and parasite is marked with dashed line and arrowheads. (K) Floral bud, with perianth lobes [L] covering the broad floral apex. Initiation of stamens (red dotted outline) and the ovary is apparent. (L) Preovarial region (dotted outline), staining pink-red. (M, N) Initial cell separation gives rise to ovarial locules. Cell wall material is pulled apart in the process (black arrows). (O) Ovarial locules with initial ovule (arrows) formation. The placenta is covered in mucilage (black dots). (P) Transverse section of morphologically secondary locule with young, undifferentiated ovules (arrows). (Q) Ovules with the nucellus still exposed. (R) Ovules with the nucellus covered by the inner integument (outer integument reduced at the base of the inner one) and micropyle curved toward the placenta. (S) Part of placenta with dense carpet of irregularly arranged ovules. (T) Longitudinal section of placentae with numerous irregularly arranged mature ovules. Bars: A, F, K, I, O = 1 mm; B, D, G, H, J, P, R–T = 200 μm; C, L–N, Q = 100 μm; E = 25 μm.

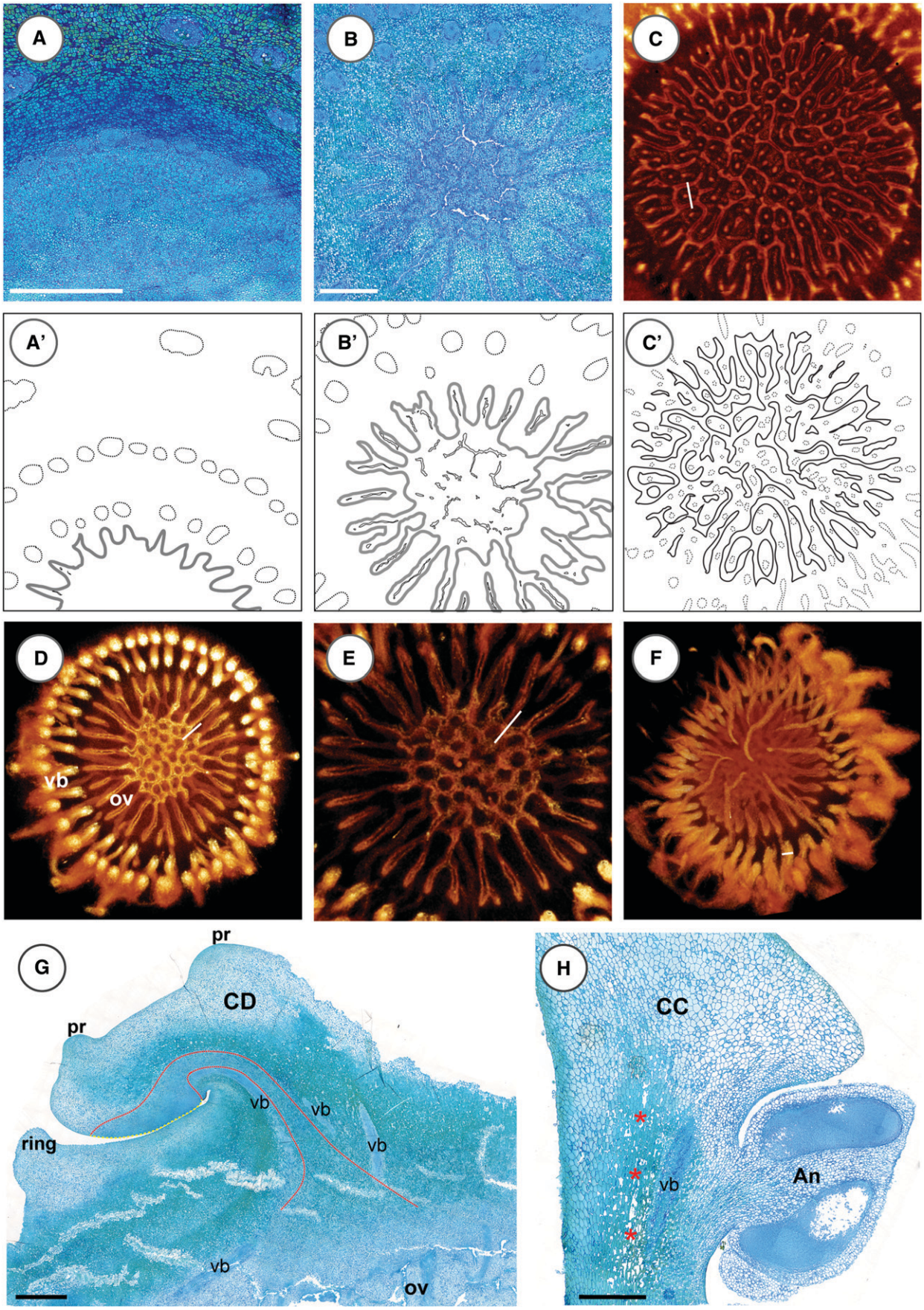
A
B
C
A'
B'
C'
D
E
F
vb
ov
G
pr
CD
pr
vb
vb
vb
ring
vb
ov
H
CC
vb
An

100% ethanol to Technovit solution. Embedded material was sectioned using a Microm (Walldorf, Germany) HM 355 rotary microtome with a conventional knife D. The 7-μm thick sections were stained with 0.05% ruthenium red (w/v) and 0.1% toluidine blue (w/v) in water and mounted in Histomount. Permanent slides of the microtome sections are deposited in the Harvard University Herbaria (A).

***Scanning electron microscopy (SEM)*—**For SEM, FAA-fixed floral buds and selected organs were dissected and postfixed in 2% OsO_4 in water for 2 h, washed three times with ddH_2O, and transferred to 100% ethanol through increasing alcohol series, then critical-point dried using a Samdri-PVT-3D (Tousimis Research, Rockville, Maryland, USA). The dried specimens were mounted on aluminum stubs and sputter-coated with Pd/Pt at 20 mA or Pt/Au at 40 mA for 180s. The stubs were examined with EVO-SEM at 10.00 keV, and image brightness and contrast were uniformly adjusted in Photoshop.

***X-ray tomography and 3D reconstructions*—**The FAA-fixed material was infiltrated with 1% phosphotungstic acid for 4 wk (with a change of infiltration solution every week) (Staedler et al., 2013). The samples were stabilized with acryl pillow foam in an ethanol atmosphere in plastic container of adequate size and scanned with an XRadia MicroXCT-200 system (Carl Zeiss, Oberkochen, Germany) comprising a 90 kV microfocus x-ray source (Hamamatsu Photonics, Hamamatsu, Japan), switchable scintillator-objective lens units, and a 2 k × 2 k CCD camera. Scanning parameters are summarized in Appendix S1 (see Supplemental Data with online version of this article). The program XMReconstructor 8.1.6599 (XRadia, Pleasonton, California, USA) was used to perform the 3D reconstruction from the scanning data. The AMIRA-based XM3DViewer 1.1.6 (XRadia) was used for the visualization of the scan data.

RESULTS

Rafflesiaceae bauplan*—Shoot apex formation*—The first conspicuous stage of a new Rafflesiaceae flower shoot within the host is a protocorm, which is a smooth, teardrop-shaped body (Fig. 2A) displaying marked basal–apical polarity such that the apex is toward the periphery of the host root. Histological differentiation, observed as parenchymatization and cell elongation, proceeds acropetally. No morphological differentiation of root or shoot is apparent at this stage. The shoot apex is formed within the apical part of the protocorm on the side toward the periphery of the host by differentiation of a thin sheet of tissue (ca. 7 cell layers thick) (Fig. 2B, C). This sheet of tissue can be defined as a front, transecting an arc of ca. 70° in longitudinal sections, which later expands laterally at both ends to form an arc of about 150°. Just below the front, to the inside of the parasite's precursor of the floral bud, a zone of cell separation forms as the layer pulls away from what will become the morphological surface of the shoot apex, transforming the protocorm into a cormus. Thus, the shoot apex of Rafflesiaceae is not derived from a primary morphological surface, making it remarkably different from the common development of angiosperms. The outer layer of tissue overlaying this newly formed apex is characterized by flat cells (Fig. 2C, D) and remains in close contact with the host tissue where it can be discerned as a thin membrane until the floral bud emerges from the host (Fig. 2D). As the shoot apex initiates its first organs, the bracts, the space between the apex, and the outer membrane becomes filled with mucilage (Fig. 2D). The resultant shoot apical meristem (SAM) lacks a typical tunica-corpus differentiation in the sense that all of the cells appear to have the potential to divide periclinally, although anticlinal divisions do predominate in the new epidermal layer (Fig. 2G). The SAM and later the floral organs are surrounded by a contact zone at the host–parasite interface where the cells are strongly tanniniferous (Fig. 2F, J). Large, vacuolated, and longitudinally oriented cells characterize the basalmost conical region of the cormus (Fig. 2F). These cells exhibit characteristic pitting of the cell wall (pit fields), indicating extensive intercellular communication in this area (Fig. 2E).

Bracts—There is no axillary bud formation, and a single flower terminates the highly compacted shoot (Fig. 1A–C). The emergence of two or more floral buds in close proximity on the host root does not signify dichotomization of the protocorm. Each individual flower originates from a separate protocorm. The flanks of each broad shoot apex produce several bracts in a Fibonacci spiral before the shoot apex is transformed into the floral apex (Fig. 2I). The bracts have a protective function and are present throughout development, covering the flower while it is inside the host and after emergence. The bracts have wide insertions, are broadly ovate, and exhibit a progression in shape from slightly notched or cordate to broad with round tips. They are crowded in bud, which often causes neighboring bracts to interlock. At anthesis, the withered and blackened bracts form a persistent crown surrounding the perianth at the base of the flower where it is connected to the host. The number of bracts in *Sapria* is generally lower (on average, 10) than in *Rafflesia* (~20) and *Rhizanthes* (~16).

Flower development—As would be expected given their final large size, the floral apex is broad (Fig. 2F, I, K). Floral organs are initiated on the flanks of the apex: the whorls of the perianth organs are initiated first, followed by a single whorl of stamens (Fig. 2K). Concomitantly with the initiation of the stamens, a ring structure appears between the whorls of the perianth and the androecium and expands to varying degree in the three genera (Nikolov et al., 2013). The gynoecium is remarkable in that no carpels are ever formed on the surface of the floral apex. The central surface of the floral apex remains undifferentiated throughout most of the floral development and eventually forms the central column in all three genera. At the same time, or soon after the initiation of the stamens, histological differentiation occurs in the deeper layers of the floral apex (Fig. 2F, K–N). A pycnotic zone, where cells degenerate and accumulate distinct droplet-like and crystalline inclusions, is formed below the meristem proper (Fig. 2F, H). Above this pycnotic

←

Fig. 3. Gynoecium structure and development in Rafflesiaceae. All panels are *Rhizanthes lowii* except for C and G (*Rafflesia cantleyi*). (A, B) Transverse sections, LM; (C–F) 3D reconstructions, computer tomography; (G, H) longitudinal sections, LM. (A) Initial stage, where cell separation has not been initiated. Interpretive line drawing (A') is below the panel (likewise for B', C'). There is a correspondence between vascular bundles (stippled gray circular outlines) and preovarial streaks (dark gray wavy outline). (B) Ovary architecture after cell separation. Peripheral radial clefts surround a central network of clefts. (C) Vascular bundles (dotted circles) differentiate within the ovary, locule outlines are in black. (D) Top view of the gynoecium, showing the correspondence between vascular bundles (the outer two rings, vb) and radial locules (inner lines, ov), which often bifurcate toward the periphery. (E) Central region of the ovary, with the innermost network of clefts. (F) Underside view of the gynoecium, showing the mesh of vascular bundles. (G) Longitudinal section of the central disk [CD] of *Rafflesia*, showing the arching PTTT (dotted red outline) and the broad stigmatic surface (dotted yellow outline); vb = vascular bundles; pr = processes; ov = ovary. (H) Longitudinal section through the central column [CC] of a male *Rhizanthes* bud, showing loosely packed tanniniferous cells (red asterisks) at the place of a pollen tube transmitting tract in female flowers; An = anther. Bars = 1 mm, except (F) = 370 μm.

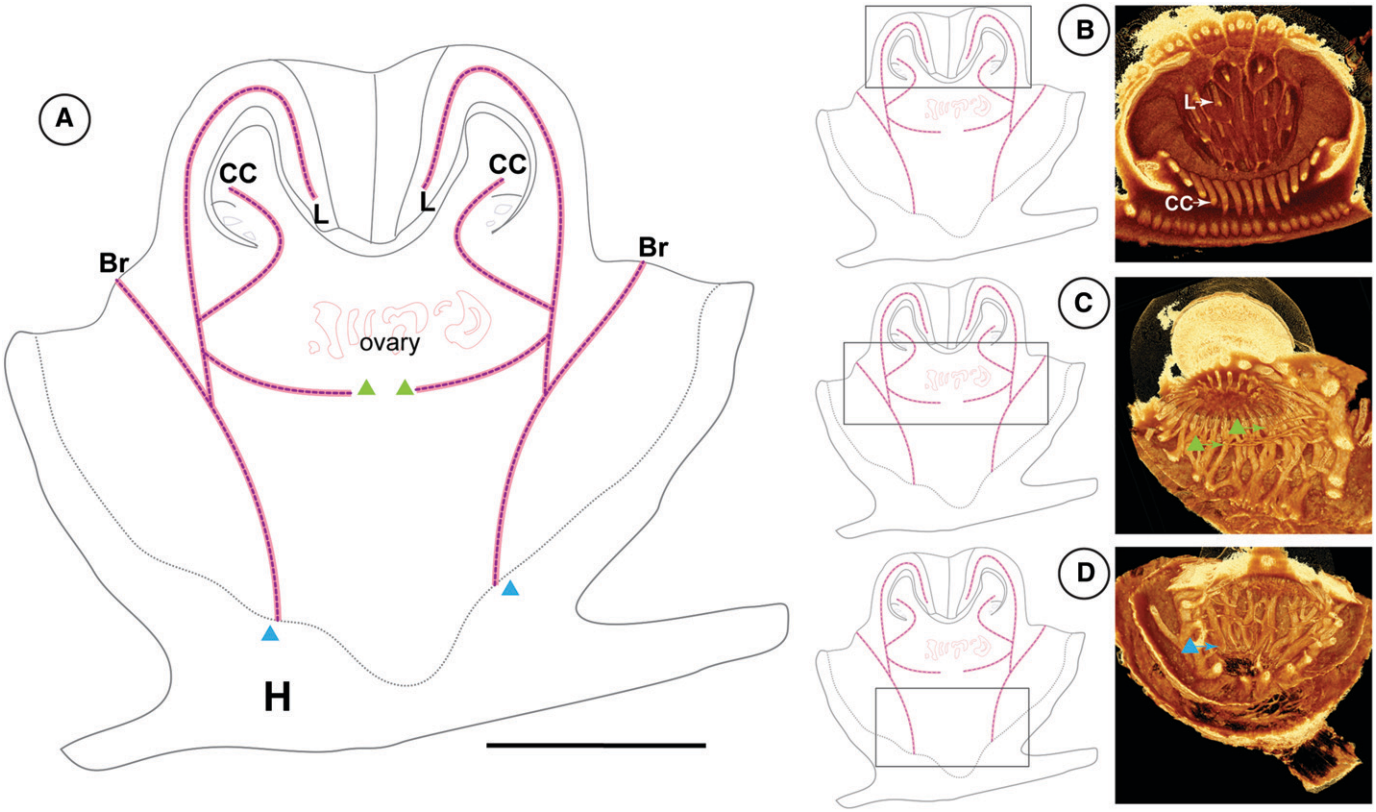

Fig. 4. Vascular architecture of *Rhizanthes* bud. (B–D) MicroCT 3D reconstructions. The connection between the host [H] and the parasite vasculature is indicated by blue triangles; free terminals below the ovary are marked with green triangles. (A) Schematic of vascularization, showing the three main branches of the vascular system, terminating in the bracts [Br], the perianth lobes [L], and the central column [CC]. The ovary is surrounded by vasculature from all sides except the top, where it connects to the pollen tube transmitting tract. (B) Vascular bundles in the perianth [L] and the central column [CC]. (C) Vascular bundles below the central column. (D) The basal region of the floral bud, showing the obconical shape of the vascular system where it connects with the vasculature of the host. Bars = 5 mm.

zone, regions with irregular outlines and distinct staining are differentiated radially from the center of the meristem toward the periphery (Fig. 2K). These regions will give rise to the locules of the ovary (Fig. 2L–N) and consist of loosely packed cells with large central nuclei and several vacuoles (Fig. 2L). They are distinct from the surrounding polygonal interstitial cells, which are in close contact with each other and have a single parietal nucleus and one large vacuole (Fig. 2L). Within the prelocular regions, cell walls become macerated and separate via schizogeny, forming distinct clefts in the tissue (Fig. 2M, N). The process of schizogeny appears to be initiated in the proximal and distal region of the presumptive ovary, progressing to the region in between until an entire locule has opened from the surrounding tissue. At later stages, cell debris and/or secretion are apparent, suggesting cell lysis (Fig. 2O). In transverse sections, the developing clefts have a radial orientation and are often forked at the periphery, forming Y- or V-shaped locules along the same radii as the vascular bundles of the central column (Fig. 3A–E). Importantly, the clefts have no apparent connection to the primary morphological surface and their internal surfaces are formed secondarily (Fig. 2M, N). In female flowers, the internal cell layer lining the locules differentiates into the placenta (Figs. 2O, 2P, 3B). The ovules are numerous and arranged irregularly (Fig. 2Q–T). At later stages of female flower development, vascular bundles differentiate within the ovary in female flowers (Figs. 3C, 5H, 5I; Appendix S2, see online Supplemental Data), and the stigmatic surface differentiates as an uninterrupted, subapical band along the circumference of the central column (Figs. 1E, 1F, 3G). The ovary makes contact with the stigma through the pollen tube transmitting tract (PTTT), which differentiates from within the surrounding compact tissue (Fig. 3G). In male flowers, the same topological position is occupied by a tissue of loosely packed tanniniferous cells (Fig. 3H).

Vascular architecture of Rafflesiaceae flowers—The flowers of Rafflesiaceae are vascularized by concentric circles of distinct vascular bundles composed of short xylem elements (cells with spiral wall thickenings); there is no wood in the parasite. The host's and parasite's conduits are in direct contact, which occurs only near the conical base of the flower shoot (Figs. 4, 5J, 7N, 7O, 9L–N). The single circle of vascular bundles that makes contact with the xylem of the host differentiates acropetally (Fig. 4A, D). Below the ovary in female flowers (or in the corresponding region of male flowers), this single vascular circle splits into two concentric circles (Fig. 4A). The irregular outer circle is diverted to vascularize the spirally arranged bracts. The inner circle splits above the region of the ovary. The outer branches vascularize the perianth lobes, reaching their tips (Fig. 4B). The inner branches vascularize the central column, where they run between the anther bases and the PTTT (or the corresponding area in male flowers) and terminate above

the attachment point of the anthers. At the point where the inner and the outer branches diverge, vascular differentiation also occurs in the parenchymatous center of the flower where free terminals run transversely and join the inner vascular circle (Fig. 4C). Thus, the ovary is surrounded by vasculature on all sides except the distal region.

Rafflesia-specific features—*Perianth*—The flowers of *Rafflesia* display an actinomorphic floral chamber with a double perianth (Figs. 1A, 5, 6, online Appendix S3). The perianth lobes (i.e., sepals) have broad insertions and are orbicular (Fig. 1A). They differ from the bracts in that they are slightly auriculate at the base at an early stage, and although they are initiated in a spiral sequence, they have a whorled phyllotaxis. As the perianth lobes grow toward the center, they may interlock but generally maintain a quincuncial aestivation (Fig. 5C). Occasionally, vestigial 6th and 7th perianth lobes are observed, which are much smaller and misshapen, suggesting that such organs could be developmental teratologies (Fig. 1A). The adaxial surface of the perianth lobes is rough and, in some species, covered by granular spots that can be of different colors (as in *Ra. cantleyi* but not *Ra. tuan-mudae*) and presumably function in pollinator attraction (Fig. 1A). The perianth lobes are tightly appressed in bud, and under dry conditions, anthesis may be impeded by a failure to overcome the adhesion among them. The congenitally fused petal whorl, called the diaphragm, is a wide, uninterrupted band in the studied *Rafflesia* species (Fig. 5D). In bud, the diaphragm is tightly appressed but not postgenitally fused to the perianth lobes. The diaphragm has a round to polygonal opening in the center, which delimitates the inner floral chamber. The abaxial surface of the diaphragm is rough and becomes imprinted by the ornamentation of the perianth lobes. Its adaxial surface is often speckled with large semitranslucent spots called "windows" (Beaman et al., 1988; Meijer, 1997), which allow light into the chamber. The diaphragm progressively tapers in thickness from its insertion point toward its edge (Fig. 6A). Although the diaphragm is not as thick as the perianth lobes, it is similarly succulent and often splits radially at anthesis due to mechanical strain. The diaphragm is vascularized similarly to the sepals, with ~45 radial vascular bundles terminating blindly at its periphery (Fig. 5D). The perianth lobes and the diaphragm are congenitally fused at their base into a campanulate perianth tube, which forms the wall of the floral chamber (Figs. 5E, 6A). The depth of the chamber varies among species. The inner surface of the tube, the adaxial surfaces of the sepals, and the diaphragm are papillate. The inner surface of the tube in particular develops conspicuous multicellular outgrowths (emergences), which are collectively called the ramenta (Fig. 6B–D). The shapes of the ramenta are diverse and species-specific. In *Ra. cantleyi*, the ramenta progress from tall, slender, and branched ramenta at the base of the floral tube (Fig. 6D) to shorter, stout, and unbranched ramenta on the walls (Fig. 6C) to flat spots on the diaphragm (Fig. 6B). Only the longer ramenta are vascularized (Fig. 6D), and their capitate ends are papillate, glistening, and appear secretory.

Central column—The base of the central column is surrounded by a ring-like structure (alternatively termed the "annulus" by Meijer, 1997). The neck of the central column is massive, cylindrical, and grooved. The grooves (known as "anther sulci") accommodate the stamens in male flowers and are much shallower in female flowers, which bear small staminodia (Figs. 5F, 6E). In male flowers, the grooves alternate with pronounced ridges lined by acicular hairs along their crests, which restrict pollinator access from the floral chamber to only one anther at a time. The grooves are densely covered by papillate hairs and ornamented by two to four streaks running parallel to the ridges, tufted with stiff, brown hairs. Distal to the grooves, the central column expands to form the central disk. A ring of stamens in male flowers and an uninterrupted stigmatic belt in female flowers occupy the lower horizontal surface of the central disk. In male flowers, the margin of the disk extends to create an overhanging edge in the shape of triangular plates that surround the stamens (Fig. 6E). The vertical edge of the central disk has a raised rim, which is lined by short hairs. In *Ra. cantleyi*, the top surface of the disk is covered with ca. 40 prominent finger-like projections called processes (Fig. 1D). The processes are massive, unbranched elaborations with wide bases. They form relatively late in development on the central disk. The larger processes at the periphery of the disk are laterally compressed and sometimes forked with variously blunt, tuberculate, or pointed ends. At anthesis, their tips are glistening and covered with fine hairs, similar to the hairs covering the raised ridge of the central disk edge. The processes are often vascularized.

The anthers of *Rafflesia* are sessile, basifixed with a broad base, globular to ellipsoidal, and hang at ca. 45° from below the disk facing inwards (Fig. 6E, F; Appendices S4, S5, S6, S7). Although the stamens are initiated as a ring of laterally elongated organs, proliferation, and expansion of the surrounding column eventually elevates and reorients them such that they become pendant and inward facing toward the column base. They have poricidal dehiscence; pollen forms a viscous slurry exuded from a single pore (Fig. 6F). Shallow grooves on the anther surface radiate out from the pore. A number of tightly packed, parallel, basally bifurcating microsporangia ("locules") differentiate inside each anther (Fig. 6F). The microsporangia are organized in approximately two circular series, which collectively converge toward the apical pore (Fig. 6F). Vascular bundles do not enter the anther, although there is extensive vascularization in close proximity to the anthers (Fig. 6G). Generally, 2–4 vascular bundles (corresponding to the 2–4 streaks in the grooves; see above) from the central column arch toward the base of the stamens, where they dichotomize forming a vascular plexus—a circumferential, uninterrupted vascular band below the base of all stamens (Fig. 6G). The plexus distally gives rise to ca. 4–7 individual vascular bundles per anther, which curve toward the vertical margin of the central disk.

Ovary—The ovary of female flowers is large and has an elaborated internal surface, organized in ~50–60 radial clefts in the periphery and an expanded network of clefts toward the center (Fig. 5I). Hundreds of thousands of randomly arranged anatropous ovules occupy the entire surface of the ovarial locules except the extreme ends of the ovary. In the male flowers examined, vestigial ovarial locules are absent and parenchyma traversed by vascular bundles occupiesthe space of the ovary.

Rhizanthes-specific features—*Perianth*—The flowers of *Rhizanthes* are actinomorphic and have two series of eight perianth lobes each, which are morphologically indistinguishable from each other at maturity (Figs. 1B, 7, 8; online Appendix S8). As is sometimes observed in *Rafflesia*, variations in the number of lobes are rare but do exist, and specimens with 15–17 perianth lobes were observed. The perianth lobes are free for most of their length and fuse toward the base to form the perianth tube (Fig. 7B–I). In bud, the perianth lobes have proximal ascending and distal descending portions (Fig. 7A). The distal portions of the perianth

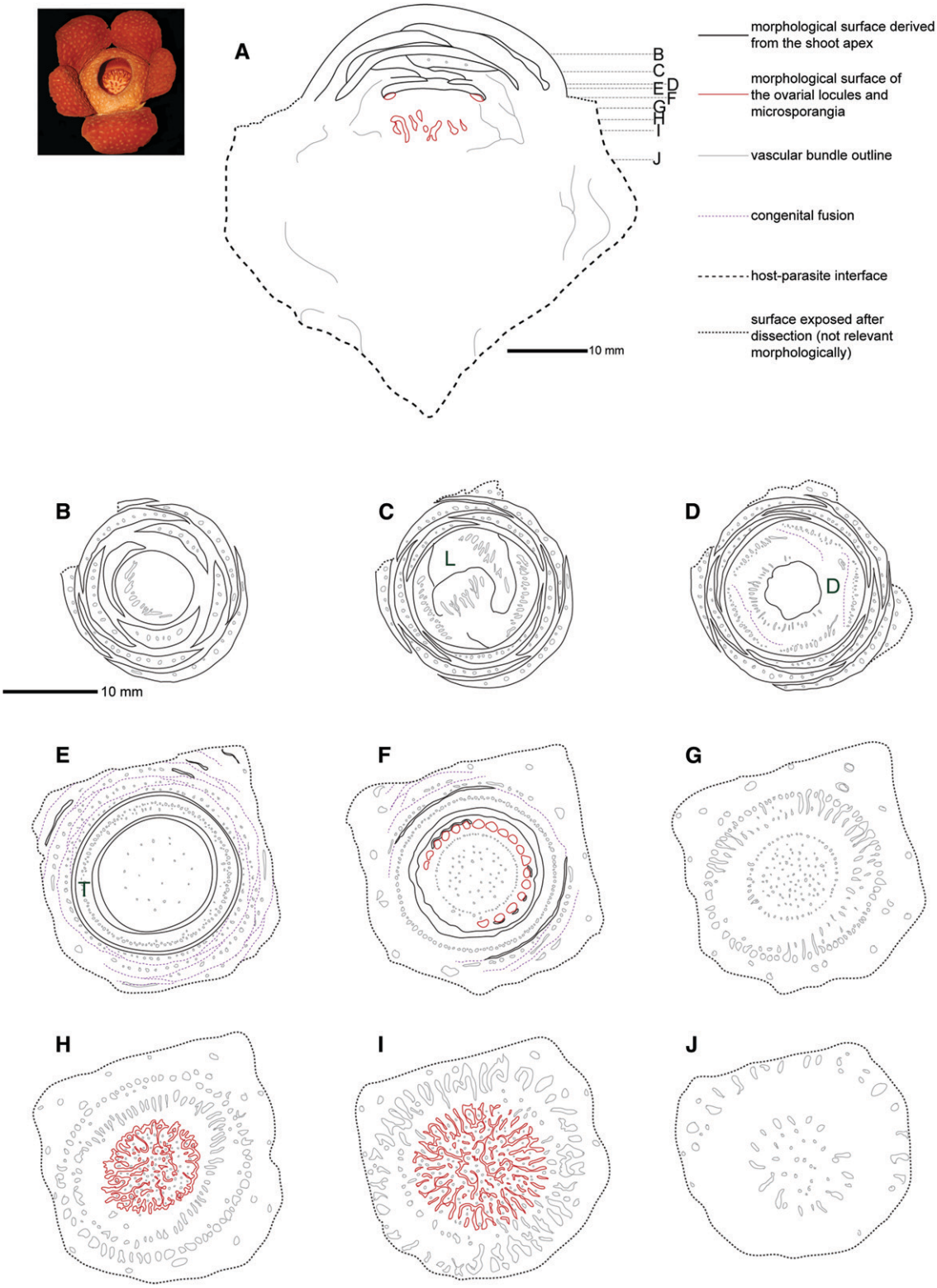

Fig. 5. *Rafflesia cantleyi*. Longitudinal section (A) and transverse sections (B–J) of female flower. Line drawings are based on microCT scanning data (Appendix S3) and histological sections. Red outlines in A, F, H, and I indicate the reproductive organs. (A) Schematic median longitudinal section indicating the relative positions of the transverse sections in images B–J. (B) Spirally arranged bracts surround the perianth. (C) Quincuncial aestivation of the perianth lobes [L]. (D) Section at the level of the diaphragm [D], showing its vascularization. (E) Level of the perianth tube [T] and the central disk, above the staminodia. (F) Level of the staminodia (red outlines). (G) Section below the attachment level of the central disk. (H) Distal end of the ovary (red outlines). (I) Midlevel of the ovary (red outlines). (J) Section below the ovary locules, showing the concentric circles of vascular bundles at the periphery of the ovary locules and the vascular bundles below the ovary.

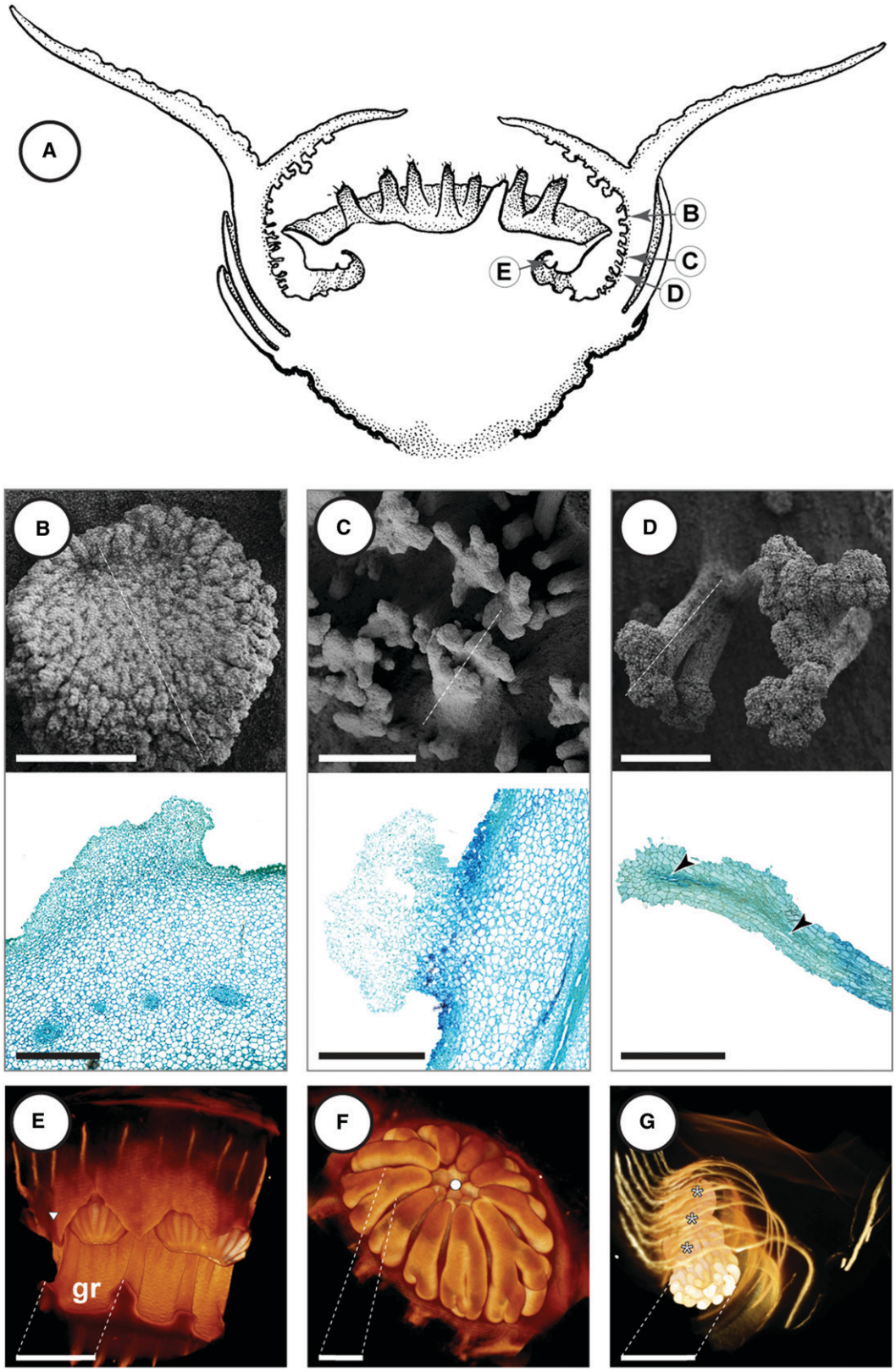

Fig. 6. Morphology and histology of *Rafflesia cantleyi*. (A) Schematic longitudinal section of open flower; circled letters illustrate topological positions of the organs and the regions depicted in subsequent panels. (B–D) Progression of ramenta elements from (B) flat blotches to (C) raised and (D) dendroid elements; dotted white lines in top SEM images mark the plane of LM sections in bottom images. (E–G) MicroCT 3D reconstructions. (E) Anthers and their corresponding grooves (gr). White triangle depicts the overhanging edge of the central disk. (F) Microsporangia of a multilocular anther, converging toward the central pore (white dot). (G) Vascular plexus (gray asterisks) at base of stamens. Bars: B–D, F = 1 mm; E = 6.1 mm; G = 4.7 mm.

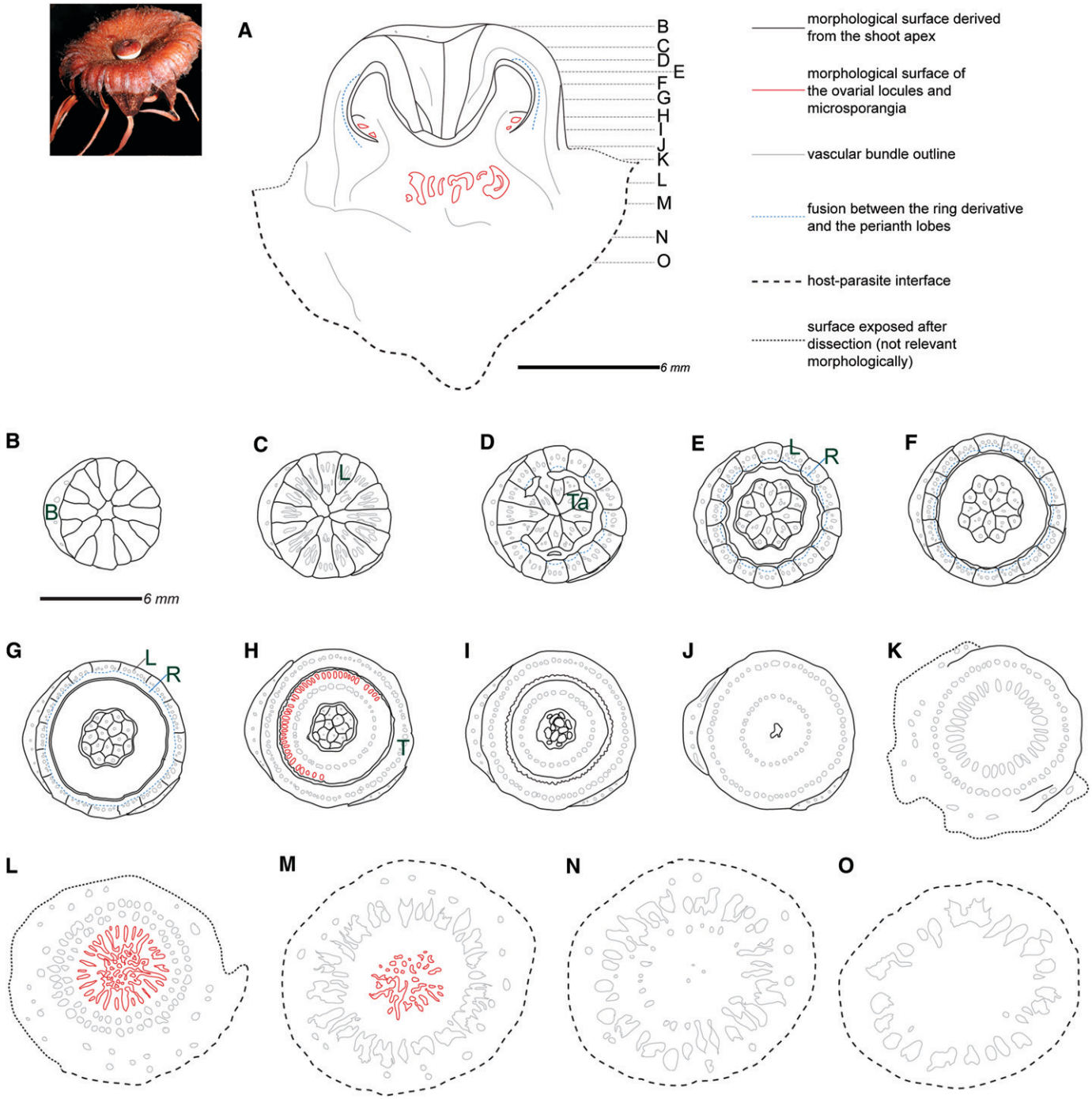

Fig. 7. *Rhizanthes lowii*, longitudinal section (A) and transverse sections (B–O) of a male flower. Line drawings are based on microCT scanning data (Appendix S8) and histological sections. Red outlines in A, H, L, and M indicate reproductive organs. (A) Schematic median longitudinal section, showing tips of perianth lobes accommodated in the depression of the center of the column. The relative positions of the transverse sections shown in panels (B–O) are indicated on the right. (B) A single bract [B] surrounds 8+8 perianth lobes. (C) Descent of the tips (tails) of the perianth lobes [L]. (D) Tails [Ta] remain coherent with each other. (E) Level of the depression of the central column, which accommodates the tails. Perianth lobes [L] are separate, and ring derivative [R] is congenitally fused (blue outlines) to their adaxial surface. (F) Central column and perianth lobes at a lower level. (G) Ring derivative [R] forms an uninterrupted band adnate (blue outline) to the perianth lobes [L]; perianth lobes are still free. (H) Level of the perianth tube [T] and the stamens (red outlines). (I) Level below the stamens. (J) Perianth tube is connected to the receptacle. (K) Receptacle of the floral bud at the attachment level of the last bracts. (L, M) Level of the ovary (red outlines). (N, O) Lower levels, where parasite vasculature becomes compacted into a ring of several massive vascular bundles.

lobes are round in cross section and stiff, and we refer to these descending portions as "tails" (Fig. 7D–H). The tails lack dorsiventral polarity and are delimited from the ascending portions of the perianth lobes by a sharp bend (Fig. 7A, D). The tails are tightly appressed in bud along their entire length (Fig. 7E–H). This adhesion can persist through anthesis, when two or more

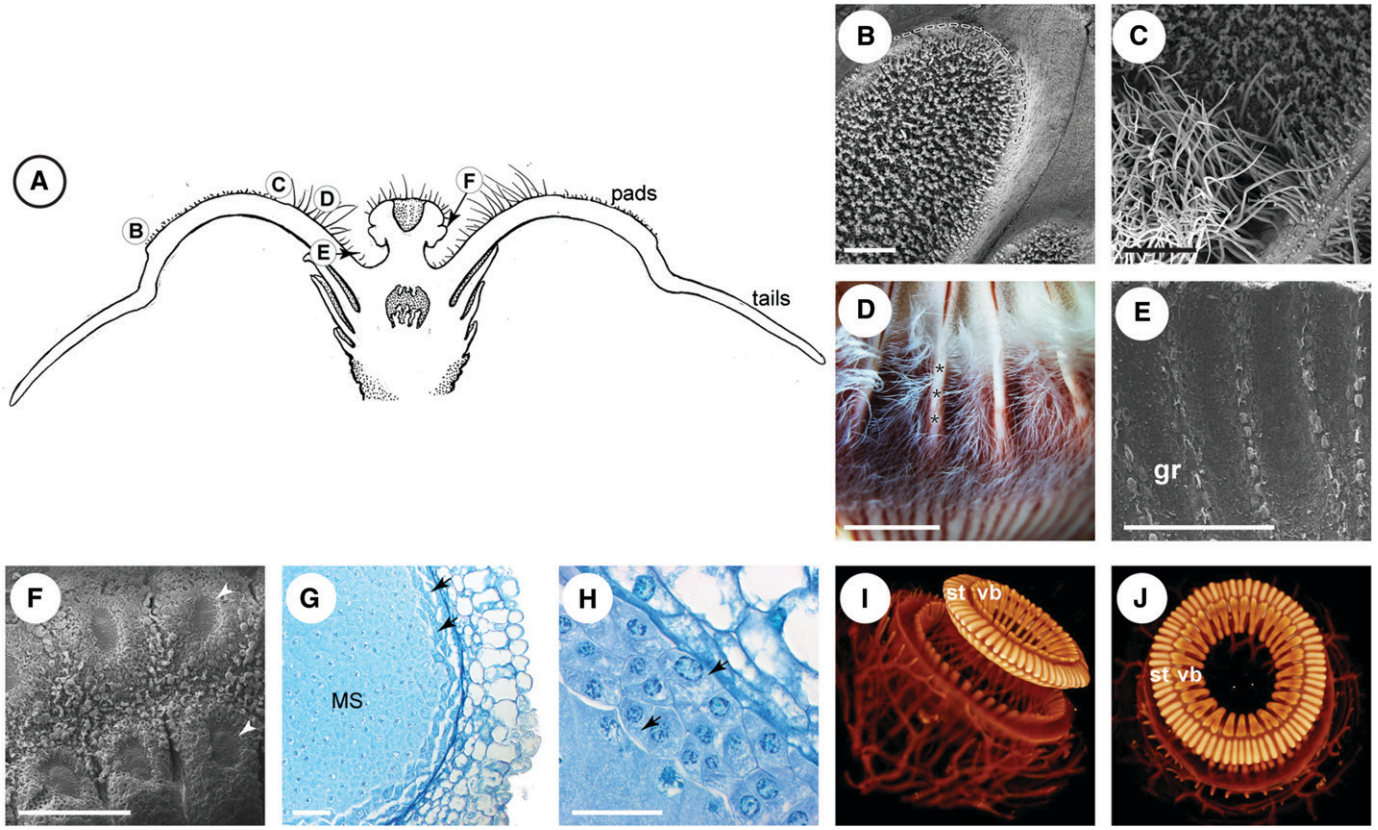

Fig. 8. Morphology and histology of *Rhizanthes*. (A) Schematic longitudinal section of an open flower of *Rh. lowii*; circled letters illustrate topological positions of the organs and regions depicted in the subsequent panels. (B) Distal end of an adaxial pad (terminating with lips, dotted white outline), covered with dendroid hairs. (C) Border between the dendroid hairs and the tuft hairs. (D) Plications (black asterisks) of the ring derivative at the border between the free perianth lobes and the perianth tube. (E) Perianth tube exhibiting low ridges, lined with a single row of trichomes, which separate shallow grooves (gr). (F) Anther dehiscence pores (white arrowheads) are arranged in two tiers. (G) Secretory tapetum, here degenerating (black arrows), lines the microsporangium [MS]. (H) Secretory tapetum (black arrows), 3–4 cell layers thick, at initial separation from the microsporocytes. (I) Two tiers of microsporangia (st) and their vascularization (vb), side view; diameter of androecial ring is 10.6 mm. (J) The two tiers of microsporangia and their vascularization, top view; the diameter of the androecial ring is 10.6 mm. Panels B, C, E, F: SEM; D: photograph; G, H: LM; I, J: microCT 3D reconstructions. Bar: B, C, E, F = 1 mm; D = 1 cm; G, H = 100 µm.

neighboring perianth lobes may be incompletely separated from each other (Fig. 1B). At full anthesis, however, the perianth lobes are reflexed, and the tails are free. The proximal ascending portions of the perianth lobes are dorsiventrally flattened and exhibit valvate aestivation in bud (Fig. 7D–F). The margins of two neighboring perianth lobes are raised where they meet (reduplicative-valvate) (Fig. 8C, D). Although the perianth lobes appear to be free from one another along their abaxial surface, along their adaxial face they are held together at the base by the thin band of the ring derivative (Figs. 7G, 8D). At anthesis, this band may split radially along its length down to the tube, but typically it retains its integrity for most of the perianth circumference. The ring-derived band extends distally to form the series of pads on the adaxial face of the ascending portion of each perianth lobe (Figs. 7D–F, 8B, 8C). A distinct margin marks the border between the perianth lobes and the pads, which terminate with a pronounced lip (Fig. 8B). In addition, the ring-derived band forms a plication in bud at the level where the perianth lobes meet the perianth tube (Fig. 8D), but this plication disappears at anthesis (Fig. 1B). At their bases, the perianth lobes are congenitally fused to form a perianth tube (Figs. 7H, 7I, 8D, 8E). The adaxial surface of the perianth tube has shallow grooves, separated by low ridges lined by a single row of short unicellular bristle-like hairs (Fig. 8E), similar to the acicular hairs lining the ridges that partition the androecium of *Rafflesia*. These ridges appear as brown streaks (Fig. 8D). The streaks bifurcate and gradually disappear distally within the tube.

Diverse trichome types are formed on the adaxial side of the perianth. The following structures are observed in the examined material. Starting from the base of the tube, there is a progression of unicellular, lignified hair types that range from short and dense "bristles" sensu Bänziger, 1996 at the tube (Fig. 8D, E), to a pronounced band of longer, unbranched hairs with tuberculate tips ("tuft hairs"; Fig. 8C, D) at the transition from the perianth tube to the free perianth lobes, to unicellular dendroid hairs on the pads ("ramenta" sensu Bänziger, 1996; Fig. 8B, C). Intermediate forms between the tuft hairs, and the dendroid hairs are observed in a narrow transition zone above the attachment of the perianth lobes (Fig. 8C). In contrast to *Rafflesia* and *Sapria*, *Rhizanthes* does not develop multicellular emergences. The tails are hairless.

Central column—The central column of *Rhizanthes* has a short, constricted base, which is wider in female flowers (Fig. 8A). Above this base, the central column consists of two portions: a lower region that bears reproductive tissue and an upper region that is sterile (Fig. 1E). The studied population of *Rh. lowii* is unisexual by

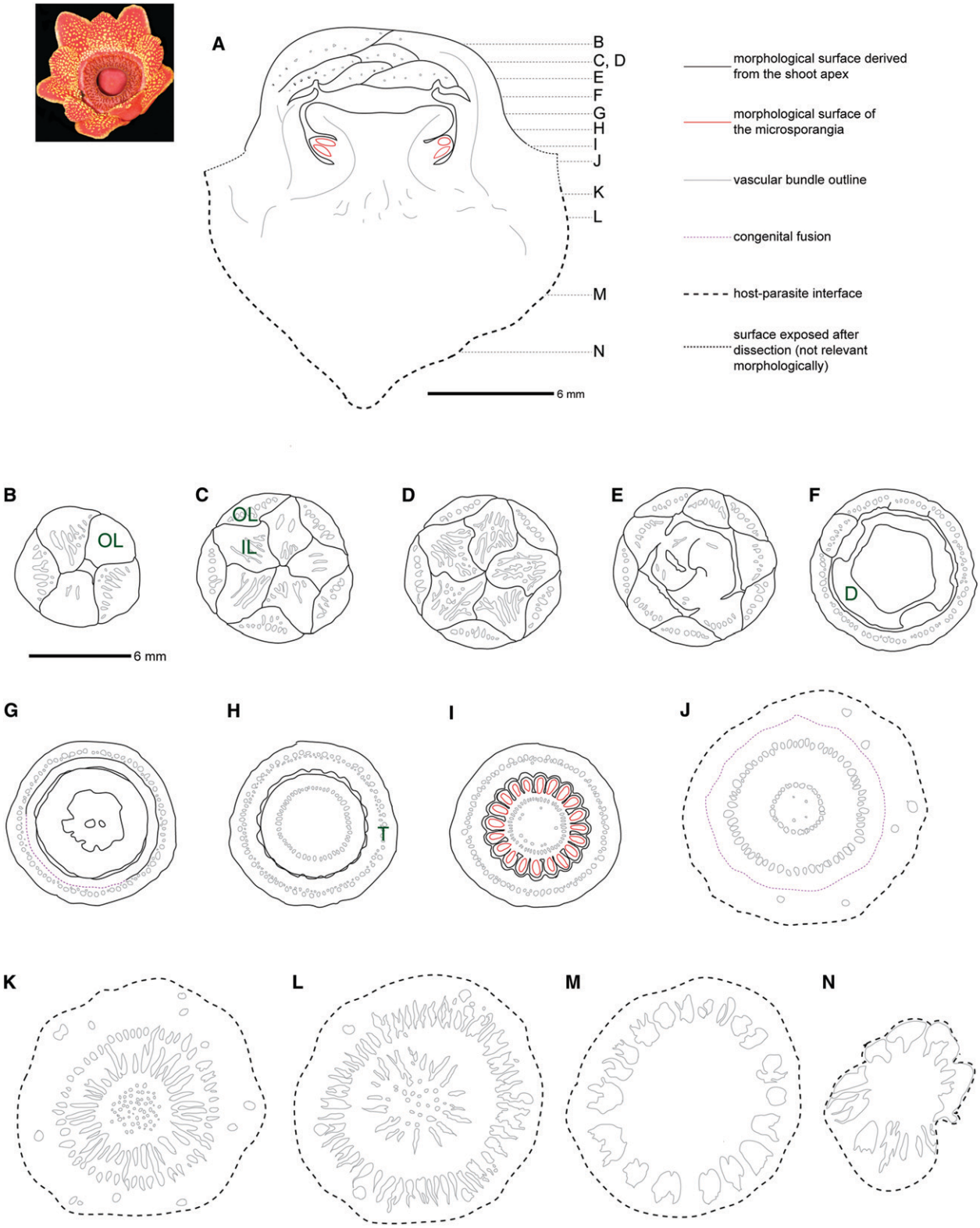

Fig. 9. *Sapria himalayana*, longitudinal section (A) and transverse sections (B–N) of male flower. Line drawings are based on microCT scanning data (Appendix S10) and histological sections. Red outlines in (A) and (I) indicate stamens. (A) Schematic median longitudinal section. (B) Imbricate aestivation of outer perianth lobes [OL]. (C–E) Contort aestivation of the inner perianth lobes [IL]. (F) Level of the diaphragm [D]. (G) Diaphragm is connected to the perianth lobes; distal part of the central column is visible. (H) Termination of vascular bundles of the central column, with the beginning of the ribs of the perianth tube [T]. (I) Level of the stamens (red outlines). (J) The perianth tube connects to the receptacle. (K–M) Vascular bundles of the floral base form concentric circles. (N) Connection of the vasculature of the parasite to the vascular system of the host.

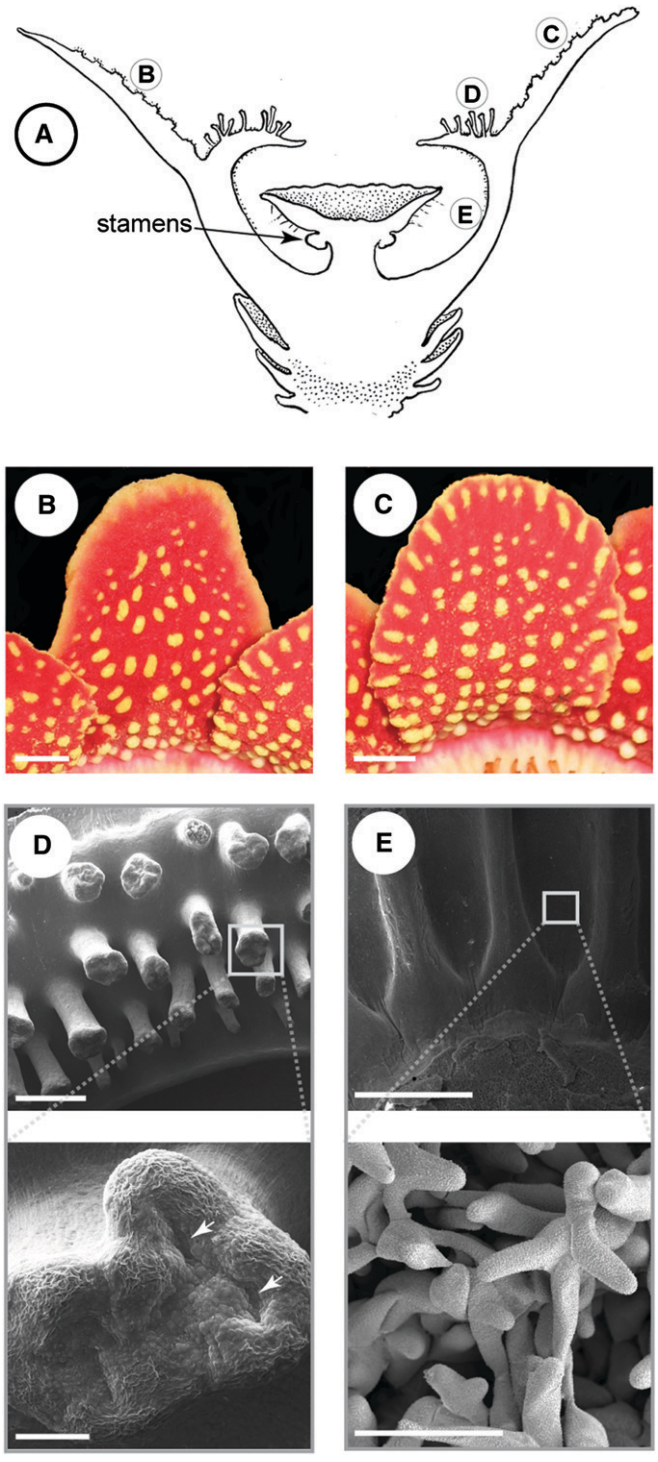

Fig. 10. Morphology of *Sapria himalayana*. (A) Schematic longitudinal section of open male flower; circled letters illustrate the topological positions of the organs and the regions depicted in the subsequent panels. (B) Outer perianth lobes have an uninterrupted yellow margin. (C) Inner perianth lobes have marginal yellow blotches. (D) Diaphragm with ramenta, SEM; apex of a ramentum with apical pores (arrows) is shown below. (E) Ridges on inner surface of perianth lobes, SEM; intertwined hairs cover the grooves between the ridges. Bar: B, C = 1 cm; D, E = 1 mm (top panels), 200 μm (bottom).

abortion so the lower portion of the column bears either a ring of anthers or the stigmatic belt (Figs. 1E, 7A, 8A). The anthers are sessile, basifixed, slightly curved, and appear laterally compressed (Fig. 8A, F). The anthers are immediately adjacent to one another, forming a continuous androecial ring (Fig. 8F, I, J; Appendix S9). Along the periphery of the ring, there are two whorls of dehiscence pores, one above the other, which correspond to two tiers of microsporangia (i.e., locules) that are lined by secretory tapetum (Fig. 8F–H). Each upper and lower microsporangium form a pair, and two such collateral pairs are vascularized by a single vascular bundle, which bifurcates before it terminates blindly in the column above the stamens (Fig. 8I, J). In female flowers, a ring of staminodia in the shape of a low crest is present below the wide, uninterrupted stigmatic belt. In both sexes, the sterile portion of the central column is concave (Fig. 1E). This depression accommodates the tips of the perianth lobe tails when the flower is in bud (Fig. 7A), and as a result, it is grooved due to their imprints. Similar imprints, left by the perianth lobes and especially the adaxial pads, are visible on the outside of the concave portion of the central column. Sparse unicellular lignified hairs cover the outside of this concave portion above the stamens and the stigma.

Ovary—The ovary of female flowers is labyrinthine with ~45 clefts radiating from an extensive central network of clefts. Its distal part is slightly concave. At the distal end of the ovary, the radial clefts converge toward, but do not connect to, one another in the center (Appendix S8). Midway through the ovary, the radial clefts merge into a central network of clefts, in which the secondarily opened space is interspersed with longitudinal strands of tissue. At the proximal end of the ovary, the radial clefts disappear, and the central network gradually fades away. Hundreds of thousands of randomly arranged anatropous ovules occupy the internal surface of the ovary. Although cleft formation and vestigial ovaries are observed in male flowers (Fig. 7L, M), the exposed surfaces do not differentiate into placenta, and no ovules are formed. The number of radial clefts in male flowers is lower (about 25–35 clefts), and the central network of clefts is much less elaborated.

Sapria-specific features—*Perianth*—The flowers of *Sapria* are actinomorphic floral chambers with a double perianth (Figs. 1C, 9, 10; Appendix S10). The sepals are quincuncial, and the petals appear contorted in aestivation (Fig. 9B–D). They are tightly appressed in bud but free at anthesis. At anthesis, the sepals and the petals display only minor ornamentation differences; sepals have a smooth, uninterrupted yellow band along the margins, whereas the margins of the petals are lined by papillate, yellow streaks that are perpendicular to the edge (Figs. 1C, 10B, 10C). These differences cannot be explained by the observed aestivation pattern. The diaphragm of *Sapria* is derived from the ring structure, and in contrast to *Rafflesia*, it is not appressed to the lobes in bud (Fig. 9A). The upper surface of the diaphragm is covered with ramenta organized in more or less concentric circles (Fig. 10D). The ramenta are clavate and have stubby protrusions at their apices. The tip of each ramentum has a depression reminiscent of an excreting pore, but secretion was not observed in anthetic flowers in the field (Fig. 10D). Toward the attachment point of the diaphragm, the ramenta elements are short, but they progressively become longer medially and then again decrease in size approaching the distal rim, which is smooth and completely devoid of ramenta (Fig. 10D). The perianth tube begins where the bases of the perianth lobes meet the base of the diaphragm (Fig. 9F, G). The perianth tube is campanulate, more so than in *Rafflesia*, and its inner surface is

TABLE 2. Summary of the major morphological characteristics of the three genera of Rafflesiaceae.

Major character	*Rafflesia*	*Rhizanthes*	*Sapria*
Floral architecture	Floral chamber (i.e., central column enclosed)	Open flower (i.e., central column exposed)	Floral chamber (i.e., central column enclosed)
Sepals and petals	Sepals are the five perianth lobes, and congenitally fused petals form the diaphragm; the sepal and petal bases are fused to form the perianth tube	Correspond to the two series (8+8) of perianth lobes	Correspond to the outer and inner perianth lobes (5+5)
Ring derivative	Ring at the base of the central column, inconspicuous at maturity	Expands to form a series of adaxial pads adnate to the perianth lobes and the perianth tube	Expands to form the diaphragm and the perianth tube
Morphological landmarks	Ramenta line the perianth tube; grooves are at the base of the central disk	A series of unicellular hairs but no true ramenta are present on the surface of the ring derivative; shallow grooves line the perianth tube	Ramenta on top of the diaphragm; grooves line the perianth tube
Central column	Expanded to form a central disk	Does not form a central disk	Expanded to form a central disk
Elaborations of the central column	Processes on top, grooves and ridges that partition the androecium at the base	Depression on top, imprints from the perianth lobes and the pads	Mostly smooth, not particularly elaborated
Anthers	Multilocular, several vascular bundles near the base of one anther	"Tetrasporangiate", 1 vascular bundle at the base of a unit of two adjacent thecae	"Tetrasporangiate", several vascular bundles at the base of a unit of two adjacent thecae

conspicuously grooved (Figs. 9H, 9I, 10A, 10E). There are 20 smooth ridges, covered by sparse unicellular hairs, which broaden distally. The grooves between the ridges are flat and covered by a dense mat of intertwined unicellular hairs (Fig. 10E). The proximal ends of the ridges are utriculate (Fig. 10E). The ridges become less pronounced and finally disappear toward the diaphragm.

Central column—The central column and disk of *Sapria* are not as robust as in *Rafflesia*. Likewise, the constricted basal portion of the central column is narrower than in *Rafflesia* but is wider in female *Sapria* flowers than in male flowers. At the intersection of the neck and the central disk, a whorl of exactly 20 stamens (in male flowers) or 20 staminodia (in female flowers) alternate with the ridges of the perianth tube (Fig. 9I). Stamens are basifixed, pendant, and facing out at an angle of ~30° to the vertical (Fig. 10A). They are ovoid and appear organized in pairs. Each stamen develops two microsporangia (locules) that converge toward a central elongated pore (poricidal dehiscence). Each stamen is vascularized by 1–3 vascular bundles, which pass near its base before terminating blindly in the periphery of the central disk (Fig. 9H, I). The central disk is umbrella-shaped, with a margin that thins toward the periphery and has a broad, shallow depression in the center. It is not elaborated except for interspersed, lignified, brown hairs that cover its surface. The stigmatic surface in anthetic female flowers, which occupies the proximal half of the lower surface of the central disk, is covered by loosely packed, broad cells with occasional tall papillae.

Ovary—Female flowers have labyrinthine ovaries composed of both radial and central clefts. Hundreds of thousands randomly arranged, anatropous ovules occupy the whole surface of the ovarial locules except their extreme ends. In the male flowers examined, vestigial ovarial locules are absent and parenchyma, traversed by vascular bundles, takes up the space of the ovary.

DISCUSSION

Our results illuminate the internal floral structure and development of Rafflesiaceae. In particular, cell separation is identified in the development of two distinct morphogenetic processes in Rafflesiaceae. The first involves the formation of the shoot apex, and the second involves the formation of the ovarial clefts of the gynoecium. Although cell separation has been implicated in shoot apex development in exceptional cases in other angiosperms (see below), its application in gynoecium development is completely novel. Because of their importance, these findings will be presented first, followed by a discussion of the functional morphology of the reproductive organs in relation to pollination. A comparison between genera is outlined in Table 2. Despite the clarified phylogenetic position of Rafflesiaceae as sister to Euphorbiaceae (Davis et al., 2007), and the progress in understanding their structural complexity (Nikolov et al., 2013), synapomorphies uniting the two families are not obvious (Endress et al., 2013). One possible example is the mostly unisexual flowers between these two families. The lack of synapomorphies is not surprising, however, given the dramatic evolutionary departure of Rafflesiaceae when compared with most autotrophic plants.

Secondary derivation of the shoot apex in Rafflesiaceae— The shoot (and floral) apex in angiosperms is covered by the primary morphological surface. It can thus be traced back to the surface of the early-stage, globular embryo (Endress, 2006). However, our data and prior observations (Brown, 1912) reveal that the shoot apex in Rafflesiaceae is formed inside the protocorm by cell separation (i.e., schizogenously) and thus represents a secondary morphological surface, where bracts and floral organs are initiated. Under this circumstance, the shoot meristem in Rafflesiaceae lacks a typical tunica-corpus organization. The functional significance of this phenomenon likely reflects the fact that the young floral apex of Rafflesiaceae grows through dense and hard host vine tissue before it emerges, similar to the root cap of a root tip pushing through the soil. In this case, this feature would serve to protect the developing floral meristem as it erupts through the host. Interestingly, a similar origin of the shoot apex has been described in the holoparasitic family Balanophoraceae (Shivamurthy et al., 1981). As in Rafflesiaceae, the shoot apex forms after lysis of a band of cells to expose a secondary surface, which then grows through the soil. A potentially similar endogenous origin of shoots is also observed in the highly specialized rheophytic family Podostemaceae, where new leaves arise below the bases of older

leaves (Rutishauser, 1997). In this case, protection of the newly developed leaves may be necessary to prevent damage from the rapidly moving water where these plants thrive.

An exceptional mode of gynoecium development among angiosperms—In the angiosperms, the continuity of the primary morphological surface, from the surface of the globular embryo to the shoot and floral apices, extends to the morphological surfaces of the gynoecium and the ovules (Endress, 2006, 2014). During gynoecium development, the primary morphological surface of the floral apex becomes complex due to differential growth and fusion. It is partly internalized after the carpel folds on itself and seals along its margins to form an internal morphological surface. However, this primary internal morphological surface always gives rise to the placenta, where ovules are borne, and it also generally marks the position of the pollen tube transmitting tract (PTTT) (Endress, 2006, 2014). This rule, which is observed in all studied angiosperms, is violated during gynoecium development in Rafflesiaceae. Rafflesiaceae instead have an internal morphological surface lining their ovary that is of secondary origin. Specifically, the ovarial cavity of Rafflesiaceae forms via cell separation (i.e., schizogenously) from within a solid mass of tissue. Thus, Rafflesiaceae have evolved an alternative form of gynoecium development that has no equivalent in other angiosperms. Gynoecium formation within solid tissue via schizogeny had previously been proposed in Rafflesiaceae (Solms-Laubach, 1876, 1898; Ernst and Schmid, 1913; Hunziker, 1926), but has not been studied in detail developmentally. However, because this mechanism is unknown in angiosperms, we tested two additional models based on the gross morphology of the female reproductive organs in Rafflesiaceae.

First, we considered a model where the inner morphological surface of the carpels could develop by early invagination from the entire primary surface of the floral apex. This invagination would have to be followed by a very early and rapid postgenital fusion of the region above the developing ovarial locules, with or without fusion among individual carpels. An example of such case (i.e., incomplete syncarpy without a compitum) is observed in *Tambourissa* (Monimiaceae) (Endress, 1980). Second, we considered a model in which the inner surface arises early from separate radial invaginations at the periphery of the floral apex, leaving a large undifferentiated center. This type of organization is known from angiosperms with numerous carpels in a single whorl, e.g., Gyrostemonaceae (Hufford, 1996; Endress, 2014). Preliminary support for this hypothesis is demonstrated by the subapical position of the stigma, the arching PTTT, and the regularity of vascular bundle arrangement around the ovarial locules in Rafflesiaceae. However, after examining numerous stages of floral development, we found no evidence of either early invagination or discrete carpel initiation on the floral apex.

From our developmental studies, the only explanation for ovary development in Rafflesiaceae is that the locules are indeed derived secondarily by way of schizogeny as proposed by Solms-Laubach (1898) over a century ago. Therefore, the gynoecium does not have a primary inner morphological surface as is the case in more than a quarter million angiosperm species. Instead, the locules and ovules are formed on a secondary surface originating schizogenously in an area where the tissue is otherwise very compact. The inferior ovary of Rafflesiaceae is thus not positioned below the receptacle via differential growth of the surrounding receptacular walls as found in angiosperms with inferior ovaries, but instead forms in situ by schizogeny. The close correspondence between vascular bundles and the radii of the ovarial locules suggests that the vascular bundles influence the position of the ovarial locules.

Why did this exceptional mechanism of ovary formation evolve in Rafflesiaceae? We hypothesize that this type of schizogenous formation may facilitate the development of extensive placental area needed to produce the nearly 1 million ovules that have been observed in these plants (Nais, 2001). Such surface area might otherwise be difficult to achieve by the usual mechanism of gynoecium formation, especially when combined with the enormous size of the Rafflesiaceae floral apex. Of course, other groups with record number of ovules and seeds, such as orchids, have unremarkable gynoecia in this regard (Endress, 1994, 2014). These groups have much smaller flowers, however, and functional correlates are difficult to draw.

Transmitting tract topology—In most angiosperms, the stigma and the PTTT develop in close association with the primary morphological surface (Endress, 2006), but the secondary derivation of the gynoecium in Rafflesiaceae poses a considerable departure from this plan. This scenario leads us to ask, what can explain the subapical position of the stigmatic belt and the arching topology of PTTT? Because the PTTT differentiates within solid tissue without the guidance of the invaginated morphological surface, it might be expected that it would follow the shortest path between the stigmatic surface and the ovary. This shortest distance would position the stigma apically, on top of the central column. Along these lines, the tips of the processes were initially suspected to contain the stigma in *Rafflesia* (Brown, 1845; Kuijt, 1969). However, the stigma in Rafflesiaceae is subapical, as first identified by Solms-Laubach (1876), and the PTTT arches in such a way that the position of the stigma in female flowers and the position of stamens in male flowers are similar. The explanation of this unexpected topology could be considered from both developmental and functional standpoints. Recently, a number of transcription factors have been shown to influence the development of the PTTT in *Arabidopsis* (Crawford et al., 2007; Gremski et al., 2007; Xing et al., 2013) and auxin-mediated patterning is implicated in at least one of these cases (Gremski et al., 2007). If the vascular pattern is a proxy of the auxin flow in the flower, it is thus not surprising that the vascular bundles in the central column are closely associated with the PTTT. Therefore, the topology of the PTTT in Rafflesiaceae may reflect an intrinsic property of the auxin flow between the base of the central column and the periphery of the central disk.

The subapical position of the stigmatic surface and the corresponding arching topology of the PTTT are also likely to be functionally adaptive. Rafflesiaceae are pollinated by carrion flies (Bänziger, 1991, 1996; Bänziger and Hansen, 1997; Pape and Bänziger, 2000). The carrion flies feed and oviposit on dead animal carcasses, which Rafflesiaceae are thought to mimic (Beaman et al., 1988; Bänziger, 1991, 1996). In male Rafflesiaceae flowers, the pollen is deposited on the back of the pollinating fly, which in female flowers makes contact with the broad band of the stigmatic surface to enhance pollination and ensure effective pollen transfer (Beaman et al., 1988). The gross superficial similarity of both sexes in Rafflesiaceae may represent a form of automimicry of the female flowers to more closely resemble male flowers to best facilitate visitation by flies to both sexes. Automimicry has been implicated in the pollination biology of other floral-chamber-bearing species, including some Araceae, where only the male phase presents pollen reward to pollinators (Bernhardt, 2000) or in flowers with different architectures, such as *Begonia* (Agren and Schemske, 1991). The pollination biology of most Rafflesiaceae is not known in detail, and it is unclear what cues are critical

for visiting by their carrion fly pollinators (Bänziger, 1991, 1996; Meijer, 1997). Answers to these basic questions are needed to provide additional evolutionary explanations for the floral morphology of Rafflesiaceae.

***Functional morphology in relation to pollination*—**The dynamic nature of the sterile floral organ evolution in the family (Nikolov et al., 2013) is mirrored by the diversity in the central column morphology, although the modifications seen in the three genera concern less the basic plan (i.e., organization sensu Endress, 1994) of the central column but more its elaboration (sensu Endress, 1994). In all three genera, the anthers are elevated above the receptacle; therefore, the central column is an androphore and not an androgynophore since the ovary is inferior. The anthers of all species in the family exhibit poricidal dehiscence, which is concordant with the fly pollination syndrome and the texture of the exuded pollen slurry. The elaborations of the central column, however, vary among *Rafflesia*, *Rhizanthes*, and *Sapria* and may have important evolutionary consequences.

In the simplest case, as seen in *Rhizanthes*, the central column does not expand laterally to form a central disk. Combined with the open floral architecture, it allows both effective pollinating and nonpollinating visitors to collect pollen from all anthers, which often leads to depletion of the pollen slurry from a single flower in less than half a day (Bänziger, 1995). Furthermore, the androecium is not protected, and if its contents are not depleted by visitors, the pollen slurry frequently gets washed out by rain (Bänziger, 1995). The only barrier between visitors and the pollen is the presence of interspersed hairs on the surface of the central column. The androecium of *Sapria* is more secluded, protected first by the closed floral chamber, and second by the expanded central column, which forms an umbrella-like central disk. In addition to protecting the pollen, the darker environment of the floral chamber is thought to trap pollinating flies, which then spend a longer time inside the flower (Pape and Bänziger, 2000). However, the whorled arrangement of the anthers and the lack of partitions between them allow pollen to be collected from all stamens, as in *Rhizanthes*.

In the largest and most species rich genus, *Rafflesia*, the column is instead modified to compartmentalize the androecium, possibly as a precaution against pollen wastage. The grooves on the central column of *Rafflesia* accommodate individual anthers, and adjacent grooves are separated by high ridges lined by stiff, acicular hairs, which do not permit access into neighboring grooves. The central disk forms overhanging flanks, which additionally isolate the inward-facing anthers, such that they are completely hidden. Thus, the specific shape of the tunnel leading to an anther, created by the grooves (floor), the ridges (side walls), and the disk (ceiling), ensures precise placement of the pollinators. This specific pollination mode may explain the higher species diversity in *Rafflesia* (~30 spp.), vs. *Rhizanthes* (3–4 spp.) and *Sapria* (3 spp.) (Bendiksby et al., 2010).

In contrast to the stamens of *Rhizanthes* and *Sapria*, which can be compared to the conventional, dithecate, tetrasporangiate angiosperm stamen, the stamens of *Rafflesia* are multilocular and athecal (Endress and Stumpf, 1990). This condition resembles other parasitic plants (e.g., *Viscum*, Santalaceae), and the autotrophic *Polyporandra* (Icacinaceae), where multiple microsporangia develop within a single anther and the anthers do not have two longitudinal dehiscence lines (Endress and Stumpf, 1990). The anthers of *Rafflesia* are quite large and may trigger the differentiation of several vascular bundles in its proximity (Sachs, 1981). Thus, the large size of *Rafflesia* likely allowed for a novel stamen organization. However, the functional significance of the multilocular anthers in *Rafflesia* is not clear. The large anthers produce abundant pollen, which requires extensive surface area for nourishment (Scott et al., 2004). In addition, the anthers might serve as dispensers of the abundant pollen slurry. The increased inner surface area of a multilocular anther likely generates an increased capillary force when compared to a tetrasporangiate anther of similar size. This capillary force may counteract the gravitational pull of a drop of pollen slurry and could limit the amount of pollen slurry exuded at a certain time, which would allow multiple pollen depositions—another precaution against pollen wastage.

Another aspect of the fly pollination syndrome concerns the mimicry of the flower to resemble decaying flesh on the forest floor. In addition to the olfactory cues, the visual and tactile cues are important to attract pollinating flies (Pape and Bänziger, 2000; Davis et al., 2008). Rafflesiaceae develop a wide array of outgrowths, both unicellular and multicellular, which are believed to mimic animal fur (Bänziger, 1996). The most distinct of the latter are the ramenta, which in *Sapria* and *Rafflesia* are multicellular and appear secretory. The secretion may be a reward for the pollinators. The ramenta of *Rhizanthes* consist of unicellular hairs, which are not secretory. The ramenta of *Rhizanthes* and the ramenta in *Sapria* and *Rafflesia* are, therefore, not obviously homologous, and the term "antler hairs" for *Rhizanthes* as suggested by Bänziger, should be preferred (Bänziger and Hansen, 2000). Nectar-like secretion is produced by glandular structures in the pads in *Rhizanthes* and is attractive to a wide array of forest dwellers (Bänziger, 1995), which is possibly an interesting case of transference of function (Baum and Donoghue, 2002). Here, the secretory function of the ramenta in *Rafflesia* and *Sapria* may have been transferred to the pads in *Rhizanthes*.

***Conclusions*—**The flowers of Rafflesiaceae have puzzled morphologists for nearly two centuries. In a previous study (Nikolov et al., 2013), combining structural and genetic investigations, we clarified the identity of the sterile organs of the flower, which surround the reproductive organs, and identified a novel sterile ring structure. Here, we focused on the reproductive organs of Rafflesiaceae, which are organized in a central column, which is differently elaborated in each of the three genera and in an inferior ovary. We also characterized the formation of the shoot apex and the gynoecium development in the family. In these two cases, the surface of the floral apex and the surface of the ovarial clefts are exposed secondarily in an extraordinary process of cell separation. The secondary formation of the morphological surface of the shoot apex has precedents in other plant groups, but secondary derivation of the inner surface of the gynoecium has not been documented in any other angiosperm. Thus, the large floral size and the endoparasitic lifestyle of Rafflesiaceae are associated not only with the innovation of unique floral organs, but also with novelty in the developmental mechanisms that generated these floral organs.

LITERATURE CITED

AGREN, J., AND D. W. SCHEMSKE. 1991. Pollination by deceit in a neotropical monoecious herb, *Begonia involucrata. Biotropica* 23: 235–241.

BALETE, D. S., P. B. PELSER, D. L. NICKRENT, AND J. F. BARCELONA. 2010. *Rafflesia verrucosa* (Rafflesiaceae), a new species of small-flowered *Rafflesia* from eastern Mindanao, Philippines. *Phytotaxa* 10: 49–57.

BÄNZIGER, H. 1991. Stench and fragrance: Unique pollination lure of Thailand's largest flower, *Rafflesia kerrii* Meijer. *Natural History Bulletin of the Siam Society* 39: 19–52.

Bänziger, H. 1995. Ecological, morphological and taxonomic studies on Thailand's fifth species of Rafflesiaceae: *Rhizanthes zippelli* (Blume) Spach. *Natural History Bulletin of the Siam Society* 43: 337–365.

Bänziger, H. 1996. Pollination of a flowering oddity: *Rhizanthes zippelii* (Blume) Spach (Rafflesiaceae). *Natural History Bulletin of the Siam Society* 44: 113–142.

Bänziger, H., and B. Hansen. 1997. Unmasking the real identity of *Sapria poilanei* Gagnepain emend., and description of *Sapria ram* sp. n. (Rafflesiaceae). *Natural History Bulletin of the Siam Society* 45: 149–170.

Bänziger, H., and B. Hansen. 2000. A new taxonomic revision of the deceptive flower, *Rhizanthes* Dumortier (Rafflesiaceae). *Natural History Bulletin of the Siam Society* 48: 117–144.

Bänziger, H., A. Lamb, and A. Kocyan. 2007. Bisexual *Rhizanthes lowii* (Beccari) Harms (Rafflesiaceae) from Borneo: First description of flowers, fruits and seeds. *Natural History Bulletin of the Siam Society* 55: 341–352.

Barcelona, J., M. Cajano, and A. Hadsall. 2006. *Rafflesia baletei*, another new *Rafflesia* (Rafflesiaceae) from the Philippines. *Kew Bulletin* 61: 231–237.

Barkman, T. J., S.-H. Lim, K. M. Salleh, and J. Nais. 2004. Mitochondrial DNA sequences reveal the photosynthetic relatives of *Rafflesia*, the world's largest flower. *Proceedings of the National Academy of Sciences* 101: 787–792.

Baum, D. A., and M. J. Donoghue. 2002. Transference of function, heterotopy, and the evolution of plant development. *In* Q. C. B. Cronk, R. M. Bateman, and J. A. Hawkins [eds.], Developmental genetics and plant evolution, 52–69. Taylor and Francis, London, UK.

Beaman, R., P. Decker, and J. Beaman. 1988. Pollination of *Rafflesia* (Rafflesiaceae). *American Journal of Botany* 75: 1148–1162.

Bendiksby, M., T. Schumacher, G. Gussarova, J. Nais, K. Mat-Salleh, N. Sofiyanti, D. Madulid, et al. 2010. Elucidating the evolutionary history of the Southeast Asian, holoparasitic, giant-flowered Rafflesiaceae: Pliocene vicariance, morphological convergence and character displacement. *Molecular Phylogenetics and Evolution* 57: 620–633.

Bernhardt, P. 2000. Convergent evolution and adaptive radiation of beetle-pollinated angiosperms. *Plant Systematics and Evolution* 222: 293–320.

Brown, R. 1822. An account of a new genus of plants, named *Rafflesia*. *Transactions of the Linnaean Society* 13: 201–236.

Brown, R. 1845. Description of the female flower and fruit of *Rafflesia arnoldi* with remarks on its affinities; and an illustration of the structure of *Hydnora africana*. *Transactions of the Linnean Society* 19: 221–239.

Brown, W. H. 1912. The relation of *Rafflesia manillana* to its host. *Philippine Journal of Science* 7: 209–226.

Crawford, B. C., G. Ditta, and M. F. Yanofsky. 2007. The *NTT* gene is required for transmitting-tract development in carpels of *Arabidopsis thaliana*. *Current Biology* 17: 1101–1108.

Cronquist, A. 1988. The evolution and classification of flowering plants. New York Botanical Garden, Bronx, New York, USA.

Davis, C. C., P. K. Endress, and D. A. Baum. 2008. The evolution of floral gigantism. *Current Opinion in Plant Biology* 11: 49–57.

Davis, C. C., M. Latvis, D. L. Nickrent, K. J. Wurdack, and D. A. Baum. 2007. Floral gigantism in Rafflesiaceae. *Science* 315: 1812.

Endress, P. K. 2014. Multicarpellate gynoecia in angiosperms: Occurrence, development, organisation and architectural constraints. *Botanical Journal of the Linnean Society* 174: 1–43.

Endress, P. K. 1980. Ontogeny, function and evolution of extreme floral construction in Monimiaceae. *Plant Systematics and Evolution* 134: 79–120.

Endress, P. K. 1994. Diversity and evolutionary biology of tropical flowers. Cambridge University Press, Cambridge, UK.

Endress, P. K. 2006. Angiosperm floral evolution: Morphological developmental framework. *Advances in Botanical Research* 44: 1–61.

Endress, P. K., C. C. Davis, and M. L. Matthews. 2013. Advances in the floral structural characterization of the major subclades of Malpighiales, one of the largest orders of flowering plants. *Annals of Botany* 111: 969–985.

Endress, P., and S. Stumpf. 1990. Non-tetrasporangiate stamens in the angiosperms: Structure, systematic distribution and evolutionary aspects. *Botanische Jahrbücher für Systematik und Pflanzengeographie* 112: 193–240.

Ernst, A., and E. Schmid. 1913. Über Blüte und Frucht von *Rafflesia*. *Annales du Jardin botanique de Buitenzorg* 27: 1–58.

Gremski, K., G. Ditta, and M. F. Yanofsky. 2007. The *HECATE* genes regulate female reproductive tract development in *Arabidopsis thaliana*. *Development* 134: 3593–3601.

Griffith, W. 1845. On the root-parasites referred by authors to *Rhizantheae*; and on various plants related to them. *Transactions of the Linnean Society* 19: 303–348.

Hufford, L. 1996. Developmental morphology of female flowers of *Gyrostemon* and *Tersonia* and floral evolution among Gyrostemonaceae. *American Journal of Botany* 83: 1471–1487.

Hunziker, J. 1926. *Beiträge zur Anatomie von Rafflesia patma Bl.* Ph.D. dissertation, University of Zurich, Zurich, Switzerland.

Igersheim, A., and O. Cichocki. 1996. A simple method for microtome sectioning of prehistoric charcoal specimens, embedded in 2-hydroxyethyl methacrylate (HEMA). *Review of Palaeobotany and Palynology* 92: 389–393.

Kuijt, J. 1969. The biology of parasitic flowering plants. University of California Press, Berkeley, California, USA.

Meijer, W. 1997. Rafflesiaceae. *In* C. Kalkman, D. W. Kirkup, H. P. Nooteboom, P. F. Stevens, and W. J. J. O. de Wilde [eds.], Flora Malesiana vol. 13: 1–42. Rijksherbarium, Leiden, Netherlands.

Nais, J. 2001. *Rafflesia* of the world. Natural History Publications (Borneo), Kota Kinabalu, Sabah, Malaysia.

Nickrent, D. L., A. Blarer, Y.-L. Qiu, R. Vidal-Russell, and F. E. Anderson. 2004. Phylogenetic inference in Rafflesiales: The influence of rate heterogeneity and horizontal gene transfer. *BMC Evolutionary Biology* 4: 40.

Nikolov, L. A., P. K. Endress, M. Sugumaran, S. Sasirat, S. Vessabutr, E. M. Kramer, and C. C. Davis. 2013. Developmental origins of the world's largest flowers, Rafflesiaceae. *Proceedings of the National Academy of Sciences, USA* 110: 18578–18583.

Pape, T., and H. Bänziger. 2000. The new species of *Sarcophaga* (Diptera: Sarcophagidae) among pollinators of newly discovered *Sapria ram* (Rafflesiaceae). *Raffles Bulletin of Zoology* 48: 201–208.

Rutishauser, R. 1997. Structural and developmental diversity in Podostemaceae (river-weeds). *Aquatic Botany* 57: 29–70.

Sachs, T. 1981. The control of patterned differentiation of vascular tissues. *Advances in Botanical Research* 9: 151–262.

Scott, R. J., M. Spielman, and H. G. Dickinson. 2004. Stamen structure and function. *Plant Cell* 16: S46–S60.

Shivamurthy, G., B. Swamy, and G. Arekal. 1981. Ontogeny and organization of the inflorescence in *Balanophora*. *Annals of Botany* 48: 853–859.

Solms-Laubach, H. 1876. Die Entwickelung der Blüthe bei *Brugmansia Zippelii* Bl. und *Aristolochia Clematitis* L. *Botanische Zeitung* 31: 481–489.

Solms-Laubach, H. 1898. Die Entwicklung des Ovulums und des Samens bei *Rafflesia* und *Brugmansia*. *Annales du Jardin botanique de Buitenzorg* 2 (supplement): 11–22.

Staedler, Y. M., D. Masson, and J. Schönenberger. 2013. Plant tissues in 3D via X-ray tomography: Simple contrasting methods allow high-resolution imaging. *PLoS ONE* 8: e75295.

Takhtajan, A., N. Meyer, and V. Kosenko. 1985. Pollen morphology and classification in Rafflesiaceae s.l. [in Russian]. *Botanicheskii Zhurnal* 70: 153–162.

Takhtajan, L. 1997. Diversity and the classification of flowering plants. Columbia University Press, New York, New York, USA.

Wurdack, K. J., and C. C. Davis. 2009. Malpighiales phylogenetics: Gaining ground on one of the most recalcitrant clades in the angiosperm tree of life. *American Journal of Botany* 96: 1551–1570.

Xing, S., M. Salinas, A. Garcia-Molina, S. Höhmann, R. Berndtgen, and P. Huijser. 2013. *SPL8* and miR156-targeted *SPL* genes redundantly regulate *Arabidopsis* gynoecium differential patterning. *Plant Journal* 75: 566–577.